Eur. Phys. J. Spec. Top. (2024) 233:1017–1036
https://doi.org/10.1140/epjs/s11734-024-01150-1

THE EUROPEAN PHYSICAL JOURNAL SPECIAL TOPICS

Review

Isomers in superheavy nuclei

D. Ackermann[1,a], S. Antalic[2,b], and F. P. Heßberger[3,4,c]

[1] Grand Accélérateur National d'Ions Lourds – GANIL, CEA/DRF-CNRS/IN2P3, Bd. Becquerel, Caen 14076, France
[2] Department of Nuclear Physics and Biophysics, Comenius University in Bratislava, 84248 Bratislava, Slovakia
[3] GSI - Helmholtzzentrum für Schwerionenforschung GmbH, Planckstraße 1, Darmstadt 64291, Germany
[4] Helmholtz Institut Mainz, Staudinger Weg 18, Mainz 55128, Germany

Received 31 January 2024 / Accepted 13 March 2024 / Published online 26 April 2024

Abstract Isomeric states in atomic nuclei are a well-known phenomenon all over the complete chart of nuclei. Their properties deliver valuable information on the structure of the nuclei. A region of specific interest are the very heavy and superheavy nuclei, where the occurrence and properties of isomeric states will have an impact on the prediction of localization and strength of the spherical superheavy proton and neutron shells. In this review, an overview of the present situation is given. Some specific features are discussed for selected examples.

1 Introduction and history

Since the prediction of the next neutron and proton shell closures beyond ^{208}Pb by Meldner [1] and Sobiczewski [2], worldwide efforts driven by the quest to find the so-called *"island of stability"* have lead to the discovery of isotopes with assigned atomic numbers of up to $Z = 118$.

Over the years, these findings have been summarized in a number of review papers, e.g., in the collection of articles [3]. Beyond the discovery of hitherto unknown elements and isotopes [4], the structure properties of these heavy nuclei play an important role, governing their decay properties [5–7] and competition against fission [8]. The quantum mechanical organization of a nucleus as an ensemble of the two types of fermions, neutrons and protons, is typically described as single-particle levels. They are defined by the eigenvalues of the nucleonic system in a nuclear potential, leading to a structure of varying density and energy gaps, defining binding energies and shell closures. One particularly intriguing nuclear structure feature is the meta-stable states. In this paper, we discuss, using selected examples, nuclear isomers being found while exploring the upper right part of the chart of nuclides (Segré chart).

In this section, we briefly introduce the special properties of the various types of isomers found in nuclei with $Z = 96$ (californium) to $Z = 110$ (darmstadtium), like, e.g., spin- and high-K isomers, and some particularities for nuclear structure features in the vicinity of the well-established deformed proton and neutron shell gaps at $Z = 108$ and $N = 152$. Additional deformed shell gaps are reported for $N = 162$ and with some evidence like in Ref. [9] $Z = 100$. The methods to experimentally study those meta-stable states will be briefly introduced in Sect. 2. We will discuss single-particle isomers in Sect. 3, K isomers in Sect. 4, and the consequence of isomeric states on nuclear stability as well as the competition between various decay modes in Sect. 5. Existing and future facilities and the opportunities offered there will be concluding the paper with Sect. 6.

In a number of review papers, the progress and achievements regarding the research in the field of nuclear isomers throughout its now more than 100-year lasting history are summarized. The historical aspects are in the focus of Ref. [12] by Walker and Podolyak.

In 1936 von Weizsäcker coined the notion of isomers in nuclei ("β-labile Kerne... in zwei 'isomeren' Sorten" - β-unstable nuclei... of two different kinds) [10], giving the example of the two activities "UZ" (later assigned

D. Ackermann, S. Antalic, and F. P. Heßberger contributed equally to this work.

[a] e-mail: dieter.ackermann@ganil.fr
[b] e-mail: Stanislav.Antalic@fmph.uniba.sk
[c] e-mail: F.P.Hessberger@gsi.de (corresponding author)

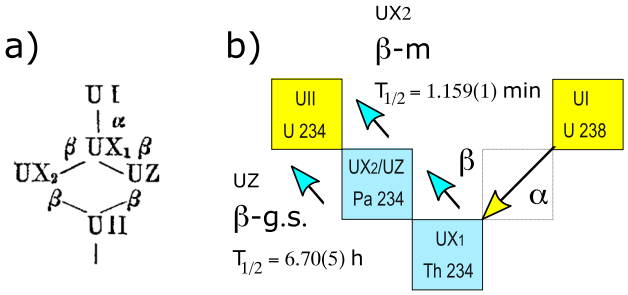

Fig. 1 The first assignment of a nuclear isomer by von Weizsäcker [10] in the β decay of ^{234}Pa observed by Hahn [11]: **a** original decay scheme by Hahn in ref. [11]; **b** decay scheme with half-lives of the two ^{234}Pa β-decay activities, from the g.s. "UZ" and the meta-stable state "UX2", and isotope assignments

as ground state of ^{234}Pa with $T_{1/2} = 6.70(5)$ h) and "UX2" (later assigned as excited state of ^{234}Pa with $T_{1/2} = 1.159(1)$ min). Hahn had assigned both to ^{234}Pa in 1921, thus observing the first nuclear isomer as shown in Fig. 1. Protactinium was the second heaviest element after uranium at that time, discovered 23 years earlier in 1913 by Fajans and Göhring [13]. As in this early case, where the spin and parity of the ground state (g.s.) and the isomer are assigned as 4^+ and tentatively as (0^-), respectively, meta-stability is caused by their quantum structure. A large difference in spin and/or K (for the definition of the K quantum number see next paragraph) delays the decay into a matching lower-energy state or g.s., leading to measurable lifetimes. For a detailed discussion of the hindrance mechanism see [14]. In this comprehensive review paper, the various aspects of nuclear isomerism are discussed as well as the role of the competing decay modes, like electromagnetic radiation/conversion-electron (CE) emission, α- and β-decay or fission. Drastic changes in shape from initial to final state can as well cause a substantial delay of the corresponding transition.

For spherical nuclei single-particle states having the same values of n (radial quantum number), ℓ (angular momentum) and j (total spin) are degenerate. For deformed nuclei, which are present in the trans-uranium region with a spatially distorted potential this is described as a function of deformation by the Nilsson model, using asymptotic quantum numbers $\Omega_\pi[Nn_z\Lambda]$ to categorize single-particle properties (see e.g. ref. [15]). The energetic sequence of states characterized by those quantum numbers at and above the Fermi energy determines the probabilities of the de-excitation scheme and transition probabilities are determined by differences in quantum number values like spin and parity of the initial and final nuclear state, determined by the unpaired nucleon(s). For well-deformed nuclei the K quantum number, defined as the sum of the total spin projection on its symmetry axis $\sum_i \Omega_i$, can be decisive for the lifetime of a state as selection rules delay its decay as a function of the difference $K_{\text{initial}} - K_{\text{final}}$ and by possible parity changes, leading to a class of meta-stable states called K isomers. In a recent compilation, Kondev et al. [16] evaluate hindrance factors (HF) and their dependence on transition multipolarities as a function of ΔK, extending the early systematics compiled by Löbner [17] in the late 1960s. Walker and Dracoulis discuss three types of meta-stability, which they categorize in shape-isomers, spin traps, and K traps [18].

2 Detection of isomers

In the region above fermium, exotic nuclei are produced usually in heavy-ion fusion–evaporation reactions. The experimental setups are designed to separate the wanted reaction products from the primary beam and to efficiently reduce the background to provide the highest sensitivity for rare events. Reaction products are typically separated based on their kinematic properties or mass, and transferred to a particle and photon detection system. In an early pioneering experiment, Dittner et al. succeeded in revealing an isomeric state with a lifetime of 15.2 ± 2.3 μs in ^{251}Fm by α-X-ray coincidences [19]. Using a rather ingenious arrangement, of a rotating wheel in combination with a set of stationary and moving detectors, the latter facing alternately the wheel and a stationary one, Ghiorso et al. found the first isomer in ^{254}No [20], by exploiting the decay recoil from the wheel onto the moving detector and subsequent recoils onto a stationary detector mounted opposite to it. They could establish a half-life of 300 ms which is close to the present value of 265(2) ms, established decades later by γ spectroscopy (see Table 1). Modern detection systems usually consist of position-sensitive silicon detectors combined with large-volume germanium detectors, providing the highest detection efficiency, e.g., $\gtrapprox 80\%$ for alpha, $\approx 100\%$ for spontaneous fission (SF) and up to 40% for low-energy γ-ray detection. Silicon detectors serve to detect α particles, electrons or fragments from SF and germanium detectors provide the possibility for the detection of emitted γ and X-ray quanta. A schematic representation of decay spectroscopy after separation is shown in Fig. 2, showing also the detection

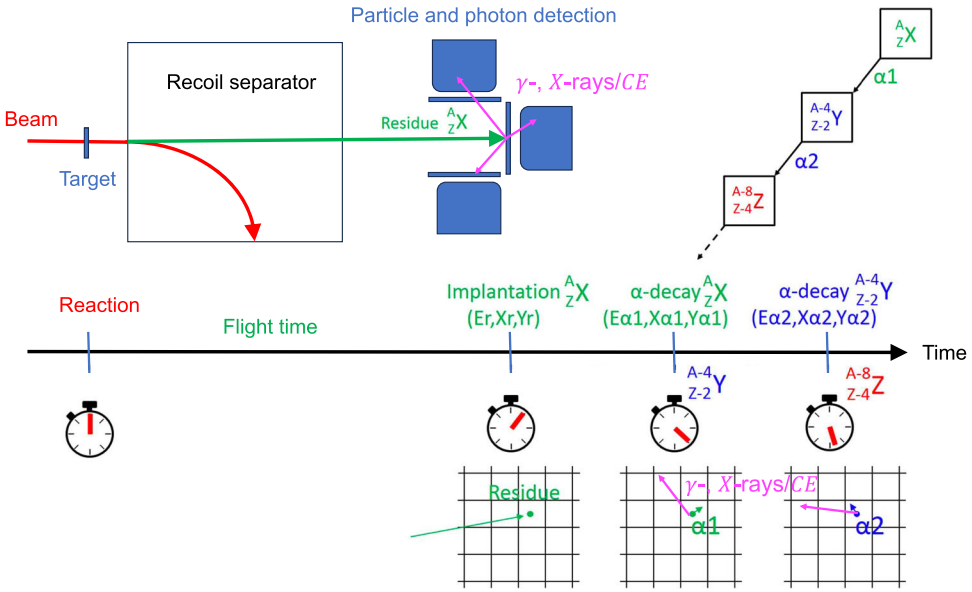

Fig. 2 Decay spectroscopy after separation and genetic correlations: the recoiling nucleus ${}^{A}_{Z}X$ is implanted in a position-sensitive detector at position (X_r, Y_r). It subsequently decays via α emission in its neighborhood at position $(X\alpha 1, Y\alpha 1)$ to the daughter nucleus $({}^{A-4}_{Z-2}Y)$ which itself decays to the granddaughter $({}^{A-8}_{Z-4}Y)$ at position $(X\alpha 2, Y\alpha 2)$. In addition to the recoils and α particles γ-, X-rays and CEs are detected in coincidence. The technique allows correlations in position and/or time of the recoil implantation and its subsequent decay due to the inclusive detection of the particles and photons involved. (Figure modified from Fig. 27 of Ref. [7])

principle of α-decay chains and genetic correlations.

The separation technique of heavy-ion reaction products is a well-established tool, proven to allow the study of very rare activities, even for single-event detection [21]. The present status and outlook toward future facilities will be given in Sect. 6. For registration and identification of individual atomic nuclei, the method of position and time correlations for implantation and decays of produced nuclei is applied in studies of the heaviest elements. The high selectivity of this method led to the reliable identification of new isotopes and elements in the region of heaviest elements, being also an efficient instrument for the identification of nuclear isomers. The methods to investigate their radioactive decay as far as α-, β-decay or SF are concerned, are generally identical to an attempt to study new isotopes and their decay. A nice example for α-decay spectroscopy of a meta-stable is the first identification of the K isomer in ^{270}Ds [22]. Combined α-γ decay spectroscopy is a powerful tool, as was shown, e.g., for ^{247}Md [23, 24], ^{255}Lr [25, 26] or ^{257}Rf [27, 28].

From the technical point of view, the identification of long-lived meta-stable states is related to the detection of their delayed radioactive decay or de-excitation process of the populated state. Apart from decaying by SF as, e.g., ^{256m}Fm or by α decay as observed for ^{266m}Hs and the aforementioned ^{270m}Ds (see Table 1, Sect. 5 and the contribution on hindrances to the α decay and fission of high-K isomers by R. Clark to this special issue), those meta-stable states in trans-uranium nuclei are mainly observed to decay by internal transitions. The de-excitation of heaviest nuclei often involves internal conversion, due to the significant increase of its probability with proton number. This process results in the emission of CEs and X-ray quanta. The position signal of the emitted electron can be used for further background suppression via the correlation to the previously emitted α particle or evaporation residue (ER) implantation signal. This is illustrated in Fig. 2 for a particle-photon detection system in the focal plane of a separator. At a given position in one pixel of the position-sensitive implantation detector, an ER is detected with its subsequent α decays and the possible, coincident emission of γ-, X-rays and CEs. One example for such a scenario is the re-confirmation of the single-particle isomer in ^{253}No in the α-decay study of ^{257}Rf [29], discovered by Bemis et al. employing delayed α-X-ray coincidences [30] and first confirmed by Streicher et al. [31, 32] in the ^{261}Sg α decay chain as well as shortly after in delayed CE spectroscopy by Lopez-Martens et al. [33]. In that fashion, employing all particle and photon correlations and coincidences, a delayed correlation search can be performed for the conversion-electron signal following the ER implantation signal to search for ER-CE events or even triple events of type ER-CE-α. Such an approach was applied for the identification of isomeric states in ^{258}Rf populated by EC decay of ^{258}Db [34].

In many cases, isomeric states are highly excited with energies well above the ground state and de-excite via a cascade of transitions. Typical examples of this kind of meta-stable states are multi-quasiparticle isomers, located usually at excitation energies above 1 MeV. Their de-excitation populates many low-energy states, which results

in a cascade of emitted γ quanta accompanied by *CE*s, both observed as a coincidence of signals in the germanium and silicon detectors. As a consequence, the method described above can be used to apply the so-called calorimetry method, where the signal of the electron cascade does not serve only as a trigger but is also used to establish an approximate excitation energy of the isomeric state. The validity of this method was proven already at the end of the 1970s [35]. In the last decades, it has been most commonly used, for example, to study K-isomeric states in the heaviest atomic nuclei [36].

Similarly, highly excited states populated by β decay in heavy nuclei de-excite by a series of internal transitions leading to a cascade of *CE*s and γ quanta. However, the possibility of investigating β decay of the heaviest nuclei is experimentally very difficult. Most of the hitherto known cases undergo β^+/EC decay with *EC* strongly dominating over the β^+ decay. Therefore, the identification of the β-decay process relies on the emitted X-ray and *CE*s from the states populated by the radioactive decay. For some cases, like for very heavy isotopes with a dominating *EC*-decay branch, the detection of such a sequence is the only source of information about the states populated by the β decay. An example is the decay of ^{253}Md leading to the identification of the $11/2^-[725]$ isomer in ^{253}Fm [37], or the first attempt to identify *EC*-decay of an isomeric state in ^{257}Rf [27].

The investigation of nuclear isomers often deals with excited states of short lifetimes. Here, one has to optimize the performance of in-flight separators. With the time of flight from the target to the focal-plane detector system in order of microseconds, they provide fast separation of the desired reaction products from the vast number of unwanted reaction products and scattered beam particles. However, in the case of such short lifetimes in the μs range, it is crucial to distinguish between signals from the implantation of *ER* and its radioactive decay. Therefore, a high time resolution of the experimental set-up is of particular importance. Concerning the decay of excited states, it is mandatory to discriminate the implantation signal or the signal of the decay populating the isomeric state and the signals from the isomer de-excitation (e.g., α decay, *EC* or *SF*). In recent years, significant advancement toward access to very short lifetimes was achieved by the application of flash-ADCs and pulse-shape analysis in so-called "digital" data acquisition systems [38], see for example, the application to isomer identification in ^{254}Rf [39] or ^{250}No [40, 41]. In the latter case, i.e., ^{250}No, this approach led to the clarification of the decay mode of the isomer, previously tentatively attributed to the long-lived *SF* branch [42, 43], with further consequences for the significant change of the *SF* hindrance factor (see Sect. 5.1 for more details).

An alternative approach to investigate nuclear isomers, even for the heaviest nuclei, is the high-precision mass measurements, e.g., in Penning traps. For a recent review of the field, see Ref. [44].

3 Spin isomers

Deformed nuclei are characterized by a high density of single-particle states. Due to the presence of orbitals stemming from high-j spherical subshells, for many isotopes orbital energies for high and low Ω differ by a few 100 keV or even by a few 10 keV only. Thus, the low energy and the large angular momentum difference to the ground state or lower-lying states lead to long lifetimes of the excited state, often on the order of several seconds. Due to the similar deformation of all nuclei in this region, we can see similar structures in nuclei with single proton states along the isotopic lines or single-neutron states along the isotone lines. In this section, we will describe two characteristic examples of odd-Z isotopes around lawrencium ($Z = 103$). In specific cases, single-particle isomers can be formed via K-hindrance which we will discuss in Sect. 4. This will be discussed there with examples for isotones with $N = 153$ neutrons (Sect. 4.1).

3.1 Isomeric states in Odd-Z isotopes

The isotopes with odd proton numbers in the fermium region are known for the presence of the low-spin single-particle Nilsson states $1/2^-[521]$ and $3/2^-[521]$ combined with higher spin states as, e.g., $7/2^+[633]$ and $7/2^-[523]$ at low excitation energies. These states are interesting since they stem from the levels $2f_{5/2}$, $2f_{7/2}$, $1h_{9/2}$ and $1i_{13/2}$ which are responsible for the existence of the possible closed shells in the region of superheavy nuclei (SHN). However, the ordering of the states is unknown for most of these isotopes and for several of them, even the ground-state configuration is not safely established.

One example is ^{247}Md, which also represents one of the most detailed studies for isotopes above $Z = 100$. It was first identified as an α emitter at the SHIP separator [47]. In a later experiment, in addition, a short-lived fission activity of 0.23 s half-life was observed and tentatively assigned to the low-lying low-spin $1/2^-[521]$ level, as for the also low-lying $7/2^-[514]$ state, a higher fission barrier was expected [48]. In follow-up studies, besides *SF*, also α emission of the 0.23-second activity was observed. Using α–γ spectroscopy, it was assigned to an isomeric state, while the $7/2^-[514]$ Nilsson level was assigned to the ground state with a half-life of 1.20(12) s [23, 24, 49]. Most of the available theoretical models predicting the single-particle level energies for odd-Z isotopes in this region expect energy differences between the levels to have only a few 100 keV [25, 45, 50]. The somehow surprising

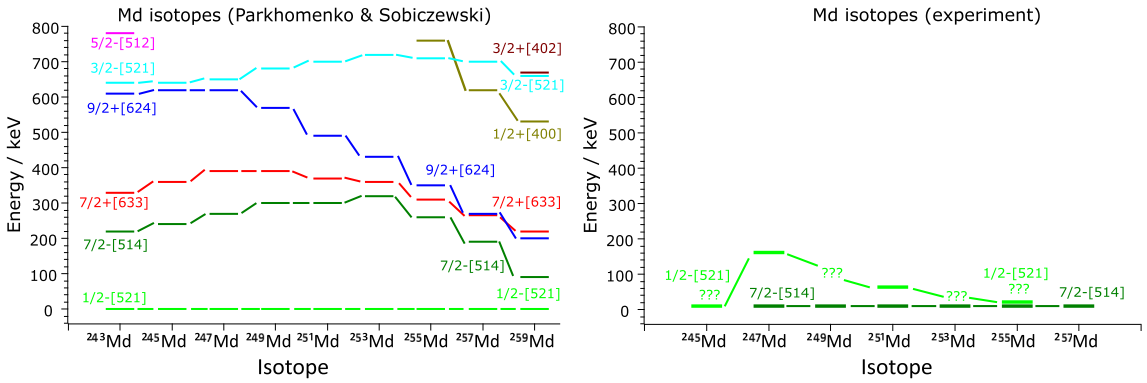

Fig. 3 Single-particle level (SPL) systematics for mendelevium ($Z = 101$) isotopes. Left panel, theoretical calculations [45]. The right panel shows available experimental data with suggested excitation energies. Please note, that for ^{245}Md, the $1/2^-[521]$ state is suggested in [46], although systematic data indicate rather the $7/2^-[514]$ configuration for the ground state

outcome of the experimental studies is that the energy difference for the identified single-particle levels goes down sometimes to several 10 keV only. As discussed in ref. [24], it raises the question of the existence of $Z = 114$ closed shell in the region of superheavy elements. In particular, the comparison of the energy difference ΔE between the two states, $1/2^-[521]_\pi$ stemming from the $2f_{5/2}$ orbital and $3/2^-[521]_\pi$ from the $2f_{7/2}$ orbital, was measured as 68 keV in ^{243}Es [24], while it is predicted to be stable at ≈ 1 MeV over a wide range of deformation, starting at the spherical $Z = 114$ shell closure, in ref. [15]. However, one has to be aware of uncertainties on both, theoretical and experimental, sides.

The pattern of a long-lived $7/2^-[514]$ ground-state and shorter-lived $1/2^-[521]$ is suggested also for neighboring isotopes ^{245}Md [46] and ^{249}Md [51]. However, more detailed information is still missing as the accumulated statistics of decay events is very low. One of the reasons is the low production cross-section of ^{245}Md. In some cases, data were collected as a part of the decay chain from heavier isotopes, as for ^{249}Md which was studied as a daughter product of ^{253}Lr and ^{257}Db. In fact, besides ^{247}Md, only for ^{251}Md and ^{255}Md excitation energies have been suggested for the isomeric $1/2^-[521]$ state relative to the $7/2^-[514]$ ground state. The ordering of the states in ^{251}Md is fixed on the basis to the α-decay fine structure data for ^{255}Lr [25].

The ground state of ^{255}Md is assigned as $7/2^-[514]$, while the $1/2^-[521]$ state is suggested at an excitation energy E^* of 12 keV [52]. Such a low-energy state should be again responsible for the existence of long-lived isomers as we see it in some neighboring mendelevium and lawrencium isotopes. The energy of this state was assumed, based on favored α decay from ^{259}Lr presumably populating a low-spin excited state, assuming the $7/2^-[514]$ configuration for the ground state of ^{259}Lr. The scenario on the population of the excited state by α decay of ^{259}Lr has been kept since early summary reports [53]. We have to note here, that the ^{259}Lr ground state is not assigned reliably even today. Some of the theoretical calculations suggest its $7/2^-[514]$ configuration [45, 50]. This scenario would lead to the conclusion that the α decay of ^{259}Lr to the ground state in ^{255}Md is unhindered. Therefore, the level assignment for the ground state and also the expected isomeric state in ^{255}Md should be taken with caution.

Even more uncertain is the situation for odd-A lawrencium isotopes. For these nuclei, in most cases, even the ground-state configuration is unknown. Presently, only for ^{255}Lr, high-quality spectroscopic data are available [25, 26], where the ground state is assigned as $7/2^-[514]$ and the isomer as $1/2^-[521]$. Contrary, the opposite order of these single-particle states was suggested for ^{253}Lr and ^{251}Lr, recently [54]. However, it should be noted, that the statistics was limited, in the case of ^{251}Lr only to several events in the work mentioned above. Based on α-decay studies of ^{261}Db and EC-decay studies of ^{257m,g}Rf, the ground-state of ^{257}Lr was tentatively assigned as $9/2^+[624]$, while a newly identified isomeric state of 0.2 s half-life was assigned to the $1/2^-[521]$ state [55].

For odd-Z isotopes above bohrium ($Z = 107$), the experimental data for nuclear isomers, available up to now, are very limited. For some isotopes, experimental data suggest broader α-decay energy distributions and slightly different half-lives. However, the results are typically based on a few events, and the statistical uncertainties do not allow any unambiguous conclusion. Although it is natural to expect the presence of similar isomeric states also in the region of the heaviest known elements, the proof of their existence would require a more substantial body of experimental data. One example of such studies and the difficulties of drawing conclusions from single events is the investigation of ^{289}Mc [56]. It would be even more challenging to obtain the necessary high-quality data to allow conclusions on the configuration of low-lying Nilsson orbitals. A boost in the capabilities of experimental instrumentation is mandatory to hope for detailed spectroscopy of the heaviest nuclei (see section 6).

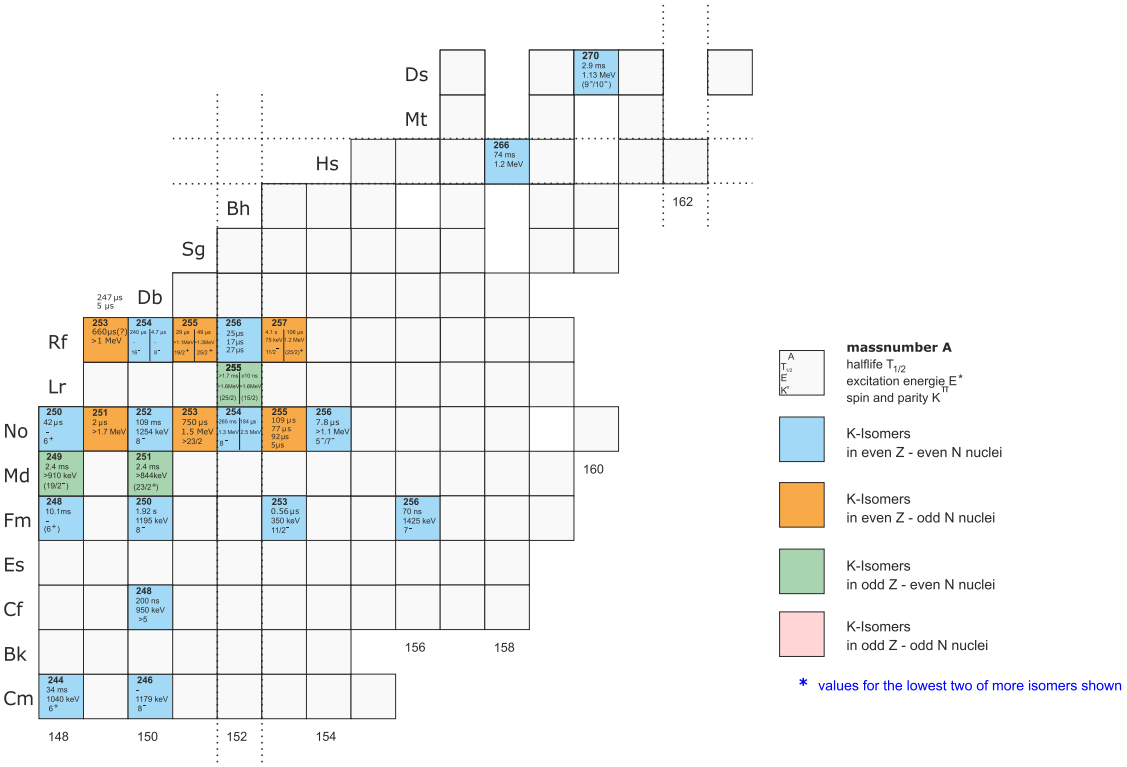

Fig. 4 Update of Fig. 43 in Ref. [7]: Summary of K isomers for the heaviest nuclei at and above $Z = 96$. For more details see Table 1

4 K isomers

In the region of the Segré chart from curium up to darmstadtium K isomers have been identified in a total of 24 nuclei (see Fig. 4 and Table 1). The access to high-J orbitals close to the Fermi energy surface in this region of deformed nuclei favors the formation of high-K values in quasiparticle excitations leading to a stabilization of the high bands and long lifetimes of high-K band heads. For a more general discussion of K isomers, see the contribution by Walker and Kondev to this special issue [57]. In the next sub-sections, we will discuss specific cases in the region of the heaviest isotopes.

After the first observation in the curium isotopes ^{244,246}Cm, even–even isotopes in the region around the $Z = 100$ and $N = 152$ and in particular ^{254}No were in the focus of a series of investigations. Only recently, K-isomeric states were found in even–odd and odd–even nuclei. According to the assignments proposed by their discoverers, they are formed by three-quasiparticle states, in contrast to the even–even cases which are supposed to have two- and four-quasiparticle configurations. In Table 1 the known K isomers in that region are listed with their major properties, including their single-particle/quasiparticle configurations. Although it is listed in a table of fissioning K isomers by Kondev et al. in ref. [16], we omit to list here a possible SF K-isomer which was tentatively assigned to ^{262}Rf by Somerville et al. [58] and which could neither be confirmed nor excluded in a later study by Lane et al. [59].

4.1 Single-particle K isomers in even-Z N = 153 isotones

For nuclei with one unpaired nucleon, the relation $\Omega = K$ is valid. So, formally, single-particle isomers in well-deformed nuclei may also be regarded as K isomers. However, such a classification seems only meaningful, if the lifetime or the decay is determined by K hindrance. The decisive relation for this is the selection rule $\Delta K = \mid K_i - K_f \mid \leq \Delta L$, where K_i and K_f denote the K value of the initial and the final state, and ΔL the difference in angular momentum which defines the multipolarity of the transition.

In the case of single-particle isomers, one has to distinguish the two cases $K_i < K_f$ and $K_i > K_f$. As the Nilsson level K_f is the head of a rotational band with spins $\Omega(= K_f)$, Ω+1, Ω+2..., in the case of $K_i < K_f$ the angular momentum difference $\Delta L = \mid K_i$-$K_f \mid$ is the lowest within the rotational band, i.e., the transition $K_i \rightarrow K_f$ has the lowest multipolarity. So, according to the definitions given above, there is no K hindrance and the transition $K_i \rightarrow K_f$ can be regarded as a usual single-particle transition.

Table 1 Extension of the table of known K isomers in heavy and SHN from curium to darmstadtium, including odd-Z/N and odd–odd isotopes and single-particle excitations with respect to earlier listings [6, 60]. IT denotes internal transitions which can proceed via γ emission or internal conversion. Note of caution: the configuration assignments in many cases are often based on systematics and model assumptions, rather than on safe experimental findings. For details of those assignments see the corresponding references

State	K^π	$T_{1/2}$	E_x	Decay mode	Configuration assignments	Ref.
^{244m}Cm	6^+	34 ms	1.040 MeV	IT	$5/2^+[622]_\nu \otimes 7/2^+[624]_\nu$	[61]
						[62]
^{246m}Cm	8^-	–	1.179 MeV	IT	$7/2^+[624]_\nu \otimes 9/2^-[734]_\nu$	[63]
^{248m}Cf	≥ 5	>140 ns	0.9 MeV	(IT)	–	[64]
^{248m}Fm	(6^+)	10.1(6) ms	–	IT	Two-quasiparticle	[65]
						[66]
						[67]
^{250m}Fm	8^-	1.92(5) s	1.195 MeV	IT	$7/2^+[624]_\nu \otimes 9/2^-[734]_\nu$	[9]
^{253m}Fm	$11/2^-$	0.56(6) μs	≈350 MeV	IT	$11/2^-[725]_\nu$	[37]
^{256m}Fm	7^-	70(5) ns	1.425 MeV	IT,SF	$7/2^+[633]_\pi \otimes 7/2^-[514]_\pi$	[68]
^{249m}Md	$(19/2^-)$	2.4(3) ms	≥0.910 MeV	IT	$7/2^-[514]_\pi \otimes 5/2^+[622]_\pi$	[69]
					$\otimes\ 7/2^+[624]_\nu$	
^{251m}Md	$(23/2^+)$	1.37(6) ms	≥0.844 MeV	IT	$7/2^-[514]_\pi \otimes 7/2^+[624]_\nu$	[69]
					$\otimes\ 9/2^-[734]_\nu$	
^{250m}No[a]	6^+	$34.9^{+3.9}_{-3.2}$	≈1.2 MeV	IT,(SF)	$5/2^+[622]\nu \otimes 7/2^+[624])\nu$	[70]
						[40]
^{251m}No	-	≈2 μs	>1.7 MeV	IT	$7/2^+[624]_\nu \otimes 9/2^-[734]_\nu$	[71]
						[72]
^{252m}No	8^-	109(3) ms	1.254 MeV	IT	$7/2^+[624]_\nu \otimes 9/2^-[734]_\nu$	[73]
						[74]
^{253m}No	$\geq 23/2$	627(5) μs	>1.44 MeV	IT	$9/2^-[734]_\nu \otimes 7/2^+[624]_\nu$	[31]
					$\otimes 7/2^+[613]_\nu$	[33]
			and/or[b]		$9/2^+[624]_\pi \otimes 7/2^-[514]_\pi$	[29]
					$\otimes\ 9/2^-[734]_\nu$	[37]
^{254m1}No[c]	8^-	265(2) ms	1.296 MeV	IT	Two-quasiparticle	[75]
^{254m2}No[c]	(16^+)	184(3) μs	≃2.5 MeV	IT	Four-quasiparticle	[76]
						[77]
						[78]
^{255m1}No	$11/2^-$	109(9) μs	240-300 keV	IT	$11/2^-[725]_\nu$	[79]
	$11/2^-$	86(6) μs	≈200 keV	IT	$11/2^-[725]_\nu$	[80]
^{255m2}No[d]	19/2-23/2	77(6) μs	1.4-1.6 MeV	IT	$1/2^-[521]_\pi \otimes 9/2^+[624]_\pi$	[79]
					$\otimes 11/2^-[725]_\nu$	
	$21/2^+$	2(1) μs	≈1.3 MeV	IT	$1/2^-[521]_\pi \otimes 9/2^+[624]_\pi$	[80]
					$\otimes 11/2^-[725]_\nu$	

Table 1 (continued)

State	K^π	$T_{1/2}$	E_x	Decay mode	Configuration assignments	Ref.
^{255m3}No[d]	$\geq 19/2$	$\geq 1.2^{+0.6}_{-0.4}\mu$s	$\geq$1.5 MeV	*IT*	-	[79]
	$27/2^+$	92(13) μs	$\geq$1.5 MeV	*IT*	$7/2^-[514]_\pi \otimes 9/2^+[624]_\pi \otimes 11/2^-[725]_\nu$	[80]
^{255m4}No	-	5(1) μs	$\geq$2.5 MeV	*IT*	Five-quasiparticle	[80]
^{256m}No	$5^-/7^-$	$7.8^{+8.3}_{-2.6}\mu$s	$\geq$ 1.1 MeV and/or[e]	*IT*	$11/2^-[725]_\nu \otimes 1/2^+[620]_\nu$ $11/2^-[725]_\nu \otimes 3/2^+[622]_\nu$	[81]
^{255m2}Lr	(15/2)	10-100 ns	>1.6 MeV	*IT*	$1/2^-[521]_\pi \otimes 7/2^-[514]_\pi \otimes 9/2^+[624]_\pi$	[82]
^{255m3}Lr[f]	(25/2)	$\geq$1.70(3) ms	$\geq$1.6 MeV	*IT*	$7/2^-[514]_\pi \otimes 7/2^+[624]_\nu \otimes 11/2^-[725]_\nu$	[83] [26] [82]
^{253m}Rf[g]	–	0.66^{+40}_{-18} ms	$\geq$ 1.02 MeV	*IT*	–	[72]
	-	$\approx$0.6 μs	–	*IT*	–	[84]
^{254m1}Rf	8^-	4.7(1.1) μs	–	*IT*, (*SF*)	$7/2^+[624]_\nu \otimes 9/2^-[734]_\nu$	[39]
^{254m2}Rf	16^+	247(73) μs	–	*IT*, (*SF*)	$7/2^+[624]_\nu \otimes 9/2^-[734]_\nu \otimes 7/2^-[514]_\nu \otimes 9/2^+[624]_\pi$	[39]
^{255m2}Rf[h]	$19/2^+$	$29^{+7}_{-5}\mu$s	1.103 MeV	*IT*	$9/2^-[734]_\nu \otimes 1/2^-[521]_\pi \otimes 9/2^+[624]_\pi$	[85] [86]
^{255m3}Rf[h]	$25/2^+$	$49^{+13}_{-10}\mu$s	1.303 MeV	*IT*	$9/2^-[734]_\nu \otimes 7/2^-[514]_\pi \otimes 9/2^+[624]_\pi$	[85] [86]
^{256m1}Rf	6,7	25(2) μs	$\approx$1.12 MeV	*IT*	–	[87]
^{256m2}Rf	10^+	17(2) μs	$\approx$1.4 MeV	*IT*	$(9/2^-[734]_\nu \otimes 11/2^-[725]_\nu)$	[87]
^{256m3}Rf	-	27(5) μs	2.2 MeV	*IT*	–	[87]
^{257m1}Rf	$11/2^-$	4.1(4) s	$\approx$75 keV	*IT*	$11/2^-[725]_\nu$	[88]
^{257m2}Rf	$(21/2^+)$	106(6) μs	1.151(11) MeV	*IT*	$1/2^-[521]_\pi \otimes 9/2^+[624]_\pi \otimes 11/2^-[725]_\nu$	[89] [88] [90]
^{266m}Hs	–	$\approx$74 ms	$\approx$1.2 MeV	α	–	[91] [60]
^{270m}Ds	9^-,10^-	$\approx$6 ms	$\approx$1.13 MeV or	α	$11/2^-[725]_\nu \otimes 7/2^+[613]_\nu$ $11/2^-[725]_\nu \otimes 9/2^+[615]_\nu$	[22] [60]

[a] Values taken from ref. [40]

[b] See Ref. [37]

[c] The configurations for the two isomers are still under debate (see corresponding references)

[d] obviously the assignments for ^{255m2}No and ^{255m3}No are inverted in Refs. [79] and [80]

[e] See Ref. [81]

[f] Values taken from Ref. [82]

[g] Note: half-lives differ by three orders of magnitude for the two literature values from [72] and [84]

[h] Configurations and the values for $T_{1/2}$ and E^* are taken from Ref. [86]

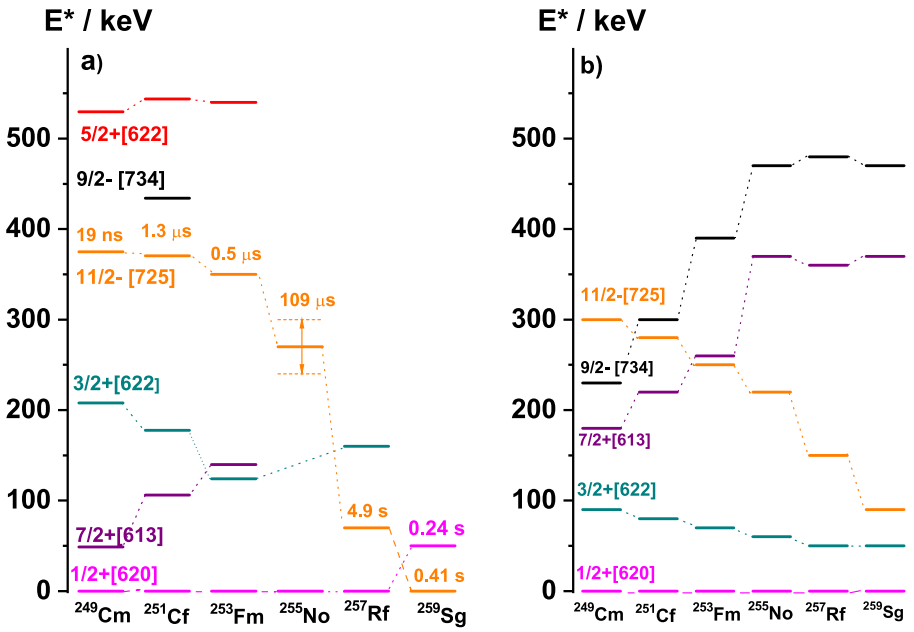

Fig. 5 Level schemes of even-Z N = 153 isotones: **a** experimental and **b** calculated [92])

Contrary to this situation in the case of $K_i > \mathrm{K}_f$ angular momenta differences into excited members of the band are $\Delta L = K_i$-K_f-n (with $n = 1, 2...$) and thus are lower than K_i-K_f. This means, that transitions of lower multipolarities from the level of K_i into members of the rotational band built on K_f are possible then for transitions into the bandhead having K_f. However, it can be shown that half-lives of those transitions are not in line with those expected for single particle transition. Representative for that kind of K isomers are the $11/2^-[725]$ states in even-Z $N = 153$ isotones.

In Fig. 5, we compare experimental levels schemes in the left panel (Fig. 5a) with the results from calculations by Parkhomenko and Sobiczewski [92] in the right panel (Fig. 5b). The ground state configurations of the $N = 153$ isotones are predicted and experimentally (except of ^{259}Sg) confirmed as $1/2^+[620]$. Low-lying Nilsson levels are $7/2^+[613]$ and $3/2^+[622]$, the trends in energy are similar, at least for the lightest nuclei in the isotonic series, while the experimental absolute energy values are shifted up for $3/2^+[622]$ and down for $7/2^+[613]$ with respect to the theoretical values. This leads to an inversion in level order for the low-Z part of the series. For the lightest member considered, ^{249}Cm, the $11/2^-[725]$ is predicted at $E^* = 300$ keV, while the experimental value was measured as $E^* = 375$ keV [93]. For this Nilsson state, the calculations show a steep decrease in energy for increasing proton numbers, while experiments show only a rather slight decrease in the range $Z = 96 - 102$. The increase of the $7/2^+[613]$ state with increasing atomic number leads to a short-lived isomeric $11/2^-[725]$ state, decaying predominantly by hindered $E1$ transitions into the $9/2^+$ and $11/2^+$ levels of the rotational band built on the $7/2^+[612]$ state. As shown in Fig. 5, a drastic change of the $11/2^-[725]$ isomer properties occurs from $Z = 102$ to 104, where the $11/2^-[725]$ eventually drops below the $7/2^+[612]$ and becomes the lowest excited Nilsson level. The change from $\Delta K = 2$ ($11/2^-[725]$, $7/2^+[612]$) to $\Delta K = 5$ ($11/2^-[725]$, $1/2^+[630]$) between the isomeric state and the lower-lying state, leads to a huge increase of the half-life by roughly a factor of 60,000. As a consequence, α decay dominates over internal transitions. A further quite interesting feature occurs from ^{257}Rf to ^{259}Sg, where the $11/2^-[725]$ Nilsson level becomes the ground state and $1/2^+[620]$ becomes the first excited Nilsson state [94]. This, formally, turns the K isomer (for ^{257}Rf) into a spin isomer (for ^{259}Sg).

4.2 High-K isomers in even–even isotopes

The heaviest nuclei for which K isomers have been detected, ^{270}Ds [22] and ^{266}Hs [60] are, as the majority of cases listed in Table 1, even–even nuclei. In both cases, the meta-stable states have a longer lifetime than the ground state and α decay of the isomer is observed, although the number of detected decays is rather small and conclusions regarding the configuration are uncertain. In Sect. 5.2, we will discuss α-decay hindrance in more detail.

The majority of K isomers observed in the region discussed here, decay by internal transition (γ/CE) for which during the past two decades a body of data has been collected which allows more systematic studies of K-isomer properties, e.g., along isotone series. This can be extremely useful to reveal and understand the nuclear structure properties leading to the formation of K isomers. As it is known for odd-mass isotones in even-Z nuclei, that nuclear structure, specifically the ordering of Nilsson levels (and also with some restrictions excitation energies) is similar along a series of isotones, similar behavior can be expected for two-quasiparticle K isomers along sequences

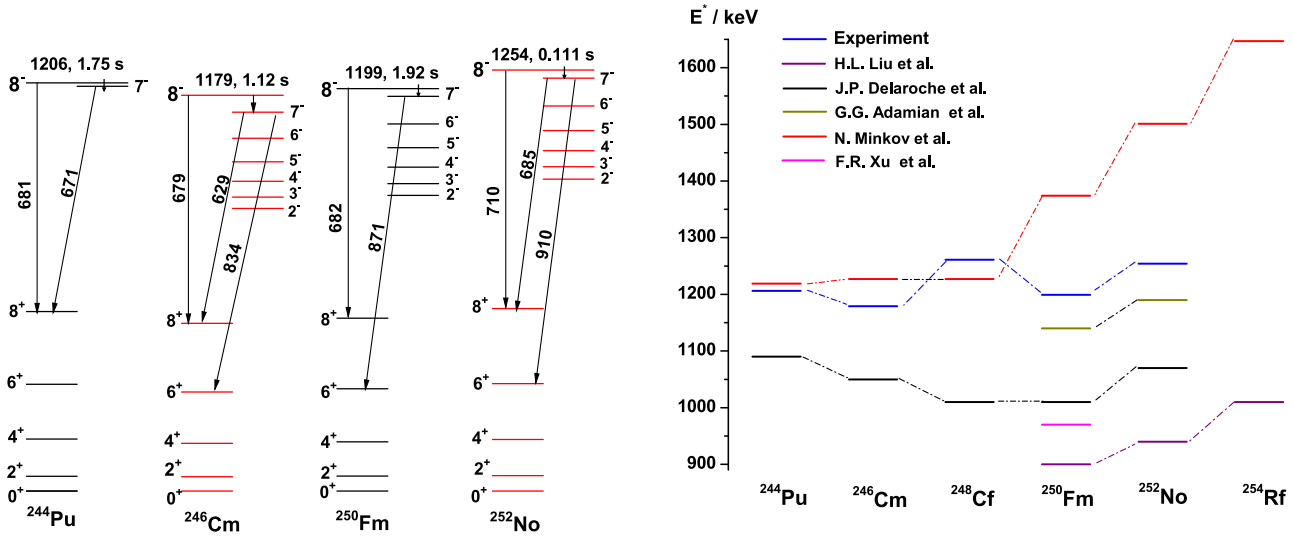

Fig. 6 Left Panel: Simplified decay schemes of K isomers in the $N = 150$ isotones ^{244}Pu, ^{246}Cm, ^{250}Fm and ^{252}No. Right panel: Comparison of predicted excitation energies of the $K^\pi = 8^-$ isomers in $N = 150$ isotones with the experimental values for the models by Liu et al. [67], Delaroche et al. [95], Adamian et al. [96], Minkov et al. [97] and Xu et al. [98]

of isotones with even neutron numbers. In $N = 150$ isotones K isomers have been identified from $Z = 94$ (^{244}Pu) to 104 (^{254}Rf). While the decay properties of ^{248m}Cf and ^{254m}Rf are uncertain, those of ^{244m}Pu, ^{246m}Cm, ^{250m}Fm and ^{252m}No are well studied, and appear to be quite similar, as shown in Fig. 6, left panel, where (for better presentation) simplified decay schemes for these isotopes are presented. For all four cases, the decay of the isomers occurs via two paths: a) decay of the isomer into the $I^\pi = 8^+$ level of the ground state rotational band which in the case of ^{252m}No is quite weak, contrary to the situation for ^{244m}Pu, ^{246m}Cm and ^{250m}Fm; b) decay of the isomer into the $I^\pi = 8^-$ level of an octupole vibrational band with the bandhead $I^\pi = 2^-$. Strong decay intensities are observed into the $I^\pi = 8^+, 6^+$ members of the ground-state rotational band, but also strong intra-band transitions followed by decay from lower members of the octupole band into lower members of the ground state rotational band are reported such as the transitions $5^- \rightarrow 4^+$ and $2^- \rightarrow 2^+$ in ^{250m}Fm [9] and ^{252m}No [73]. All these findings hint to the same structure of the isomers and presently there is common agreement on a two-quasineutron state $9/2^-[734]_\nu \otimes 7/2^+[624]_\nu$ resulting in $I^\pi = 8^-$. For the cases of ^{250}Fm [9] and ^{252}No [74], this configuration was clearly deduced from the $M1/E2$ intensity ratios for transitions within the rotational bands built up on the isomers.

Low-lying two-quasiparticle states in even-Z, $N = 150$ isotones have been addressed by a number of authors applying different model approaches [67, 95–98]. In Fig. 7, left panel, the results from Delaroche et al. [95] for two-quasineutron states are compared with the experimental data for the $N = 150$ isotones in the range $Z = 94 - 102$. In all cases the $I^\pi = 8^-$ state is the lowest lying one. Other states are predicted at $E^* > 1500$ keV. The $I^\pi = 8^-$ states, however, are predicted at somewhat lower excitation energies with $\Delta E(\text{exp,theo}) = 115 - 190$ keV, except for ^{248}Cf where the difference is $\Delta E(\text{exp,theo}) = 250$ keV. But here one should keep in mind that the excitation energy of the isomer is not well established.

In Fig. 7, right panel, we compare the two-quasiproton states predicted by Delaroche et al. [95] below $E^* = 2$ MeV with the experimental results. As expected for nuclei with different proton numbers, with consequently different single-particle levels at the Fermi surface, the predicted two-quasiproton states have different configurations, so no common trend is observed as in the case of two-quasineutron states. Therefore, the similar structure of the observed K isomers in the $N = 150$ isotones supports their interpretation as two-quasineutron states.

Calculations for K isomers in $N = 150$ isotones were also performed by Xu et al. [98], Adamian et al. [96], Liu et al. [67] and Minkov et al. [97]. Xu et al. consider as a possible configuration of the K isomer in ^{250}Fm a two-quasiproton state of $I^\pi = 7^-$ (configuration $7/2^+[633]_\pi \otimes 7/2^-[514]_\pi$) at a calculated excitation energy of $E^* = 1.01$ MeV. Note: the paper of F.R. Xu et al. was published before ^{252m}No was discovered and before detailed spectroscopic data for ^{250}Fm were published. In ^{252}No, the $I^\pi = 8^-$ was established at a considerably higher excitation energy of $E^* \approx 1.5$ MeV. Xu et al., however, remark that their calculations show that $I^\pi = 8^-$ two-quasineutron states (configuration $9/2^-[734]_\nu \otimes 7/2^+[613]_\nu$) exist systematically in $N = 150$ isotones at excitation energies around 1 MeV. But only for ^{250}Fm, a definite value of $E^* = 0.97$ MeV is given.

In Fig. 6, right panel, the experimental excitation energies of the K isomers in the $N = 150$ isotones are compared with the results of the different calculations for $I^\pi = 8^-$ two-quasineutron states. The calculations of J.P. Delaroche et al. reproduce the trend of quite stable excitation energies quite well, but deliver in general by

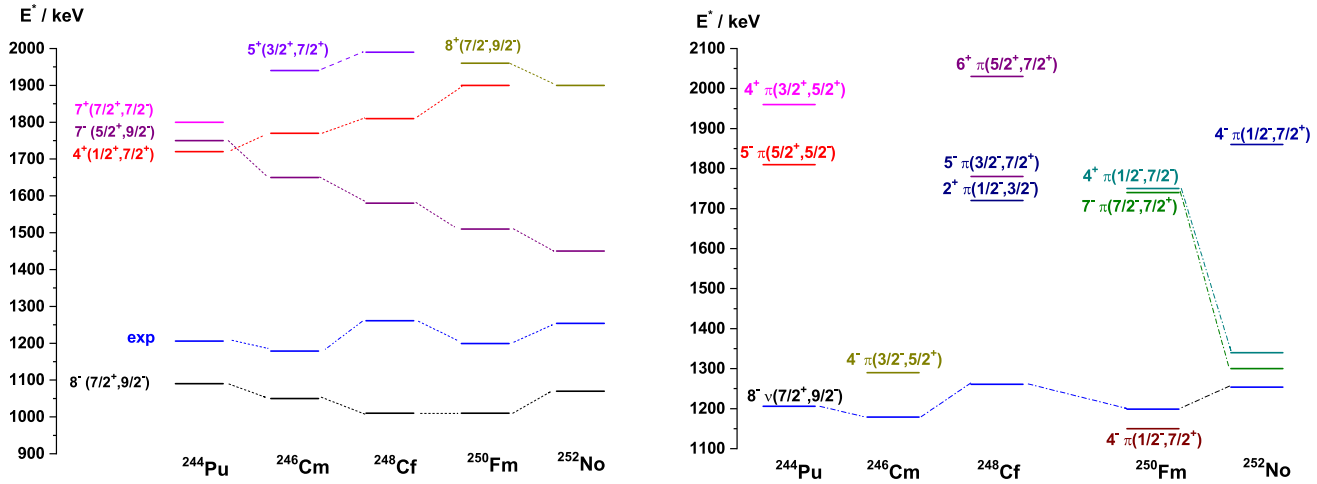

Fig. 7 Left panel: Comparison of predicted [95] excitation energies of two-quasineutron states in $N = 150$ isotones with the experimental values for the $K^\pi = 8^-$ isomers. Right panel: Comparison of predicted [95] excitation energies of two-quasiproton states in $N = 150$ isotones with the experimental values for the $K^\pi = 8^-$ isomers

about 115 – 190 keV lower values. The calculations of Minkov et al. produce quite stable excitation energies for ^{244}Pu, ^{246}Cm and ^{248}Cf and reproduce the experimental values very well within $\Delta E = |50|$ keV. But for the $Z > 98$ isotones, the calculations result in steeply increasing excitation energies and deliver excitation energies which are too high by ≈ 175 keV for ^{250m}Fm and ≈ 250 keV for ^{252m}No. Quite satisfying agreement between experimental and calculated values is obtained by Adamian et al., while Xu et al. and Liu et al. obtain too low excitation energies for the cases they consider.

The model predictions of Liu et al. may hint to a change in the structure of the K isomers going from $Z = 102$ to 104. The drastic change in the half-lives from ^{252m}No to ^{254m}Rf has been discussed in Sect. 4.1. In Ref. [39] as a possible reason, David et al. reported a decrease of the hindrance of the $M1$ decay branch from the $K^\pi = 8^-$ isomer into the $I^\pi = 7^-$ of the octupole band (indeed we observe in ^{252m}No a strong increase of the transition $K^\pi = 8^- \rightarrow I^\pi = 7^-$ (or $I^\pi = 6^-$) compared to the $E1$ transition $K^\pi = 8^-$ to the $I^\pi = 8^+$ state of the g.s. rotational band compared to the lighter isotones) and/or that the $K^\pi = 8^-$ isomer and the $I^\pi = 8^-$ might be very close in energy, leading to an accidental configuration mixing resulting in a shorter half-life.

The calculations of H.L. Liu et al. result in a clear separation of the $K^\pi = 8^-$ isomeric state (there denoted as $\nu^2 8_1^-$) from other states, like $\pi^2 7^-$, $\nu^2 6^+$ in ^{250m}Fm or $\nu^2 6^+$, $\pi^2 5^-$ in ^{252m}No. Contrary to that, in ^{254m}Rf the $K^\pi = 8^-$ state lies close in energy to a $K^\pi = 5^-$ two-quasiproton state (configuration $1/2^-[521]_\pi \otimes 9/2^+[624]_\pi$) and a $K^\pi = 8^-$ two-quasiproton state (configuration $7/2^-[514]_\pi \otimes 9/2^+[624]_\pi$). Thus, a change of the configuration of the isomeric state from ^{252m}No to ^{254m}Rf could be one reason for the drastic change in the half-lives. Another one might be the location of the $K^\pi = 5^-$ state below the $K^\pi = 8^-$ isomer, resulting in a lower hindrance of the decay due to a lower value of the difference ΔK. Two more possibilities are discussed in [39]: a) a decrease in the hindrance in the $M1$ decay branch to the 7^- member of the octupole band with increasing atomic number in the $N = 150$ isotones, and, b) the $I^\pi = 8^-$ member of the $K^\pi = 2^-$ octupole band could be very close in energy to the $K^\pi = 8^-$ isomer, leading to an accidental mixing and thus shorter lifetime. More detailed studies are necessary to clarify the situation.

Instead of fusion–evaporation reactions, the use of nucleon transfer is an alternative route to populate excited states in heavy nuclei. It was even proposed as a possible production scheme for SHN (see, e.g., Refs. [99–101]). Recently, R. Orlandi et al. [64] reported on an excited state in ^{248}Cf produced in the transfer reaction ^{249}Cf(^{18}O,^{19}O)^{248}Cf, discussing a number of configurations suggesting as most probable spins and parities K=5$^-$ to K=8$^-$ for this state. From not observed decay of this level, they deduce that its lifetime should be larger than ≈ 200 ns.

4.3 K Isomers in even–odd/odd–even isotopes

In addition to high-J, quasiparticle excitations in the presence of an unpaired nucleon coupling to three-quasiparticle configurations can lead to multiple formations of high-K states as shown by recent findings for even–odd and odd–even nuclei in the vicinity of $N = 152$, like ^{255}No and $Z = 100$ like ^{249,251}Md (see Fig. 4) which we have chosen to discuss in the following from the five even–odd (orange in Fig. 4) and three odd–even (green in Fig. 4) known isotopes for which K-isomerism was reported. An example for the single-particle level structure

around $Z = 100$ and $N = 152$ for ^{255}No shown in Fig. 9 with possible excitation scenarii illustrates the possibilities to construct the high-K configurations mentioned above.

Bronis et al. revisited data taken earlier at the velocity filter SHIP of GSI, considering *CE*s emitted by the ^{255}No ERs formed in the production reaction [79]. On the basis of $ER–CE_1(–CE_2)(–\gamma)$ correlations, the presence of two new high-K isomers, ^{255m2,255m3}No, in this even–odd nobelium isotope are proposed. The tentative level scheme of ^{255}No with the approximate location in excitation energy E^*, and possible spin and parity assignments is shown in Fig. 8a. Here, also alternative scenarios are shown for the connection of the higher lying ^{255m2}No and ^{255m3}No to ^{255m1}No, the lowest in E^* of the three isomers. In Fig. 9, a possible assignment for ^{255m2}No is illustrated based on single-particle level (SPL) configurations showing the g.s. and possible proton and neutron single-particle excitations. For ^{255m2}No Bronis et al. propose with $1/2^-[521]_\pi \otimes 9/2^+[624]_\pi \otimes 11/2^-[725]_\nu$ the same configuration as the one assigned to ^{257}Rf in the literature, for which the decay scheme is also shown in 8b. A similar situation is observed for the even–even nuclei ^{252}No and ^{250}Fm, where for both the configuration $7/2^+[624]_\nu \otimes 9/2^-[734]_\nu$ is assigned to the observed K isomer. The difference between the two configurations is that only neutron states contribute to the quasiparticle configurations for ^{255m2}No and ^{257}Rf, while for the pair ^{255}No-^{257}Rf, two of the three coupled states are proton states. In an independent experiment, the same nucleus has been investigated at the velocity separator SHELS of FLNR/JINR in Dubna, Russia [80].

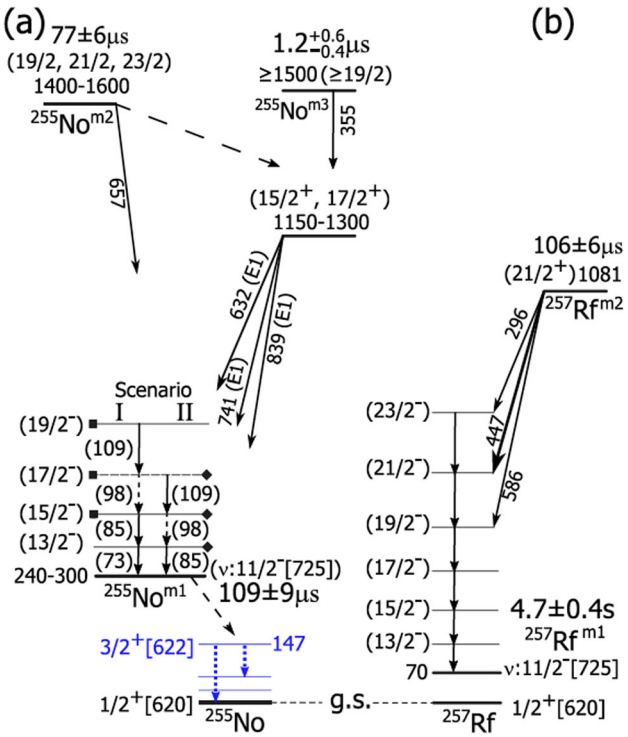

Fig. 8 **a** Tentative decay scheme of isomeric states in ^{255}No. Blue dotted lines represent previously observed levels and transitions [102]. Dashed lines indicate only tentative assignments. Roman numerals and rectangles at the end of horizontal lines correspond to different scenarii, where various members of the $11/2^-[725]$ rotational band are populated via the 632-, 741-, and 839-keV transitions (see Ref. [79], Sec. IVB). **b** Decay scheme of the isotonic neighbor ^{257}Rf [90]. Energies are in keV. (Figure and caption taken from Ref. [79].)

Fig. 9 Ground-state configuration of ^{255}No and tentative ^{255m}No three-quasiparticle configuration. Given single-particle levels for protons and neutrons were calculated in ref. [15] with nuclear deformations taken from ref. [103]. The neutron Nilsson levels 1/2+[620], $3/2^+[622]$, and $5/2^+[622]$ were placed based on the experimental results from refs [34, 104], [102], and [94], respectively. (Figure and caption taken from ref. [79].)

For ^{249}Md, the possible existence of an isomeric state was first proposed by Heßberger et al. [51] based on the α-decay population scheme from two different states in ^{253}Lr. A recent series of experiments was conducted at the gas-filled separator RITU of the cyclotron accelerator laboratory of the University of Jyväskylä. In this context, Briselet and co-workers reported on in-beam spectroscopy results for ^{249,251}Md collected with the RITU target area detection system for electron and γ spectroscopy SAGE [105, 106]. These mendelevium isotopes were produced, employing targets of ^{203,205}Tl in the reactions ^{203,205}Tl(^{48}Ca,2n)^{249,251}Md. In continuation of this study, Goigoux et al. reported hitherto unobserved K isomers in ^{249,251}Md [69], revealed in the same experiment series, using the combined silicon-germanium detector array GREAT in the RITU focal plane. They investigated the decay of these two isotopes by means of recoil-α-CE-γ coincidences. For ^{249}Md a short-lived activity of 2.4(3) ms with a lower excitation energy limit of $E^* \geq 910$ keV could be established from recoil-α-e$^-$ correlations. For ^{251}Md a state of 1.37(6) s half-life and a lower excitation energy limit of $E^* \geq 844$ keV was found applying the same method, however, with the need of the condition of a subsequent α detection in addition to the recoil-e$^-$ correlation, due to the slower decay time overlapping partly with random correlations.

For the assignment of the new meta-stable states to K isomers formed by three-quasiparticle states, the authors use a microscopic–macroscopic (MM) model as described by Muntian et al. [107] based for the macroscopic component on a Yukawa-plus-exponential folding function [108] and on a deformed Woods-Saxon single-particle potential for the shell correction energies [109]. For both isotopes, the resulting proton configuration is the same with the unpaired proton in the highest occupied SPL $7/2^-[514]$. With 148 and 150 neutrons, respectively, ^{249}Md and ^{251}Md are two and four neutrons short of the $N = 152$ shell gap. Thanks to this, they grant access to the three SPLs below the shell gap. Similar to Fig. 9 for ^{255}No, a schematic view of the single-particle configurations is given in Fig. 12 of ref. [69]. Two model approaches within the MM model framework, one using a level blocking scheme and a second one applying a quasiparticle method (for details see [69] and references therein), provide consistent arguments to extract energy and spin/parity arguments for the assignment of the SPLs involved in the three-quasiparticle configuration. For both nuclei the combination of the unpaired proton in its original g.s. level, and breaking the pair in the last occupied neutron level and elevating one of the neutrons into the next higher level turns out to be the most likely configuration for the respective K isomer. This leads to $\pi\nu^2$=$19/2^-$ with $7/2^-[514]_\pi \otimes 5/2^+[622]_\pi \otimes 7/2^+[624]_\nu$ and $\pi\nu^2$=$23/2^+$ with $7/2^-[514]_\pi \otimes 7/2^+[624]_\nu \otimes 9/2^-[734]_\nu$ for the new three-quasiparticle K isomers in ^{249}Md and ^{251}Md, respectively (see Table 1).

These examples for K isomers in even–odd and odd–even nuclei illustrate the rich nuclear structure features offered by the combination of the presence of high-J orbitals and an unpaired nucleon. Up to now, no K isomer has been reported for a system with an odd proton and an odd neutron number at the same time, in the region we are discussing here. Interesting candidates would be ^{258}Db for which two activities haven been observed in α decay as well as recently in β decay [34, 110] and its α-decay daughter ^{254}Lr, building with α- and β-decay branches a decay network around the deformed neutron shell gap $N = 152$ in the vicinity the $Z = 100$ nucleus ^{252}Fm.

5 Discussion on the impact of isomers on the stability of isotopes

5.1 Stability of K isomers against fission

It is well known that SF of nuclei with odd numbers of protons and/or neutrons is hindered compared to even–even nuclei. This feature qualitatively can be understood by the conservation of angular momentum and parity. While a pair of nuclei coupling their angular momenta to $L = 0$ may change the nuclear level at crossing points for increasing deformation toward the fission configuration, thus following the energetically most favorable path [111], for an unpaired nucleon this is normally not possible as it has to keep its angular momentum, which leads to an effective increase of the fission barrier, in literature denoted as "specialization energy", and thus to an increase of the half-life [112]. Quantitatively, this increase can be expressed by a hindrance factor $HF = T_{sf}(\text{exp})/T_{ee}$, where $T_{sf}(\text{exp})$ is the experimental half-life and T_{ee} the unhindered half-life, usually taken as the geometric mean of the half-lives of the neighboring even–even nuclei.

While the effect of fission hindrance itself is well established, it remains an open story whether there is any dependence on spin and fission-barrier height. It was suggested, that the fission-barrier height should be effectively lower for isotopes with an unpaired nucleon in a low-spin single-particle state [50]. This argument was applied for example in the case of the configuration assignment for a short-lived single-particle state undergoing fission in ^{245}Md [46]. This idea was confirmed later in the studies of ^{247}Md concerning the $1/2^-[521]$ isomer [23, 24]. However, the recent debate on different isomer decay schemes for ^{253}Rf [72, 84, 113] shows the relevance and a need of clarification for a possible quantum mechanical origin of fission hindrance. Besides the spin value itself, the pairing, the slope of the relevant single-particle orbitals and their consequent crossings along the path to the scission point might play a significant role in influencing the fission probability.

In odd–odd nuclei with an unpaired proton and an unpaired neutron, both nucleons have to keep their angular momenta, leading to even higher hindrance factors than obtained for odd-mass nuclei. Consequently, only very few cases of *SF* of odd–odd nuclei are known. For a more exhaustive discussion, see [8].

For K isomers, where pairs of nucleons are broken and the nucleons are excited into different levels, the situation resembles that in odd–odd nuclei, i.e., a strong hindrance of *SF* can be expected. So, far, only for two cases, ^{256m}Fm [68] and ^{254m}No [78] spontaneous fission was observed. In some nuclei (^{254}Rf, ^{250}No), two fission activities were observed, with the shorter-lived one attributed to the ground-state decay and the longer-lived one to the decay of the isomer. In all these cases, however, it was shown, that the isomer decays by internal transitions into the ground state, which then undergoes *SF*. Following these results, the *HF* of the K-isomer in ^{250}No, previously assumed to have a dominant fission branch [42], was suggested as $HF > 10^4$ [41].

To obtain information about the fission hindrance of K isomers, F.P. Heßberger et al. [78] performed for the case of $^{254m1,\,m2}$No some basic calculations to estimate fission half-lives of these isomers. The calculations were based on the empirical description of fission half-lives suggested by V.E. Viola and B.D. Wilkins [114]. The estimated fission hindrance factors were ≈ 1370[1] for the two-quasiparticle state ^{254m1}No and $\gtrapprox 3.2{\times}10^6$ for the four-quasiparticle state ^{254m2}No. In a later study by J. Khuyagbaatar, a significantly shorter theoretical half-life of 0.94 ms for ^{254m1}No was estimated [115], leading to the hindrance factor around 1.4×10^6. The hindrance factor reported in [78] seems significantly lower, possibly due to the use of a too low value for the barrier curvature energy. It should, however, be noted that barrier curvature energies calculated, using the modified Viola-Wilkins description, depend not only on the fission half-lives but also on the model-dependent fission barriers, resulting in a quite different barrier curvature energies and, hence, in quite different hindrance factors. A more exhaustive discussion of the problem was recently presented by F.P. Heßberger [116]. In a recent study, A. Lopez-Martens et al. [113] did not observe fission events that could be attributed to the decay of ^{254m1}No. They obtained an upper limit of $2.26{\times}10^{-5}$ for the fission branch of ^{254m1}No, meaning that fission hindrance is even at least an order of magnitude higher than discussed above.

Considering this last result, one can conclude that fission of ^{254m1}No is more hindered than typically for nuclei with one unpaired nucleon. A comparison with odd–odd nuclei is hardly possible, as there are only two cases of odd–odd nuclei where direct fission is reported, ^{262}Db (a less certain case) and ^{260}Md. In the case of ^{262}Db, a quite low hindrance factor ($HF \approx 3250$) is obtained; while for ^{260}Md, a quite high value ($HF \approx 9.2{\times}10^8$) is obtained (see ref. [8]). Thus, one may conclude that the fission hindrance of the two-quasiparticle K isomer (with two unpaired nucleons) indeed rather resembles the case of odd–odd nuclei with each, one unpaired proton and neutron. At present state, such a conclusion is indeed still somewhat speculative and more experimental information, as well as efforts from theory, are required to calculate fission half-lives of K isomers. However, it is evident, that the hindrance of spontaneous fission might play an important role in the synthesis of new isotopes and elements, where the border of stability was reached due to the extremely large fission probability. An example, where the fission dripline was reached is the region of short-lived rutherfordium and nobelium isotopes with half-lives as low as a few 10 μs [42, 117]. However, as will be shown in the next section, multi-quasiparticle K isomers might provide a stabilization effect also for other decay modes [98].

For a more detailed discussion, see the contribution on hindrances to the α decay and fission of high-K isomers by R. Clark to this special issue.

5.2 Alpha-decay hindrance for K isomers

The hindrance factor for α decay is very sensitive to the change in nuclear structure between initial and final states. However, there have been very few cases studied for multi-quasiparticle isomers until now. Some examples can be found in even–even isotopes. One of the cases is the α decay from ^{254m1}No. The α decay of the high-K isomeric state to the ground state or any low-spin low-energy state would require a significant change of angular momentum. For example, a decay from the K isomer with $K, J = 8$ to the ground state, having $K, J = 0$, the $\Delta L = 8$ would cause a significant increase of the effective barrier which would strongly hinder such a decay. On the other hand, the α decay could rather populate any matching state of the g.s. rotational band and proceed via de-excitation through the rotational band toward the ground state. However, besides the increased hindrance due to the change of the angular momentum, and thus the effective increase of the barrier, there is an expected influence on the preformation probability of the α particle. Such a decrease in preformation probability could lead to an additional hindrance from a few tens to a few thousands [118]. Other examples of α-decaying K isomers are with ^{266}Hs and ^{270}Ds the heaviest nuclei for which this type of meta-stable states has been observed [22, 60]. Also, here, we would refer to the contribution on hindrances to the α decay and fission of high-K isomers by R. Clark to this special issue, for a more detailed discussion.

[1] We realized a typo in our publication [78]; the hindrance factor for spontaneous fission of ^{254m1}No should rather be HF $\approx$ 1370 instead of HF $\approx$ 370.

6 Outlook and opportunities at future facilities

The success of nuclear structure studies and, in particular, the investigation of isomeric states for the heaviest nuclei relies on the major instrumentation, necessary to perform this type of investigations: high-intensity heavy-ion accelerators, and efficient and selective separators combined with comprehensive particle and photon detection systems. High beam intensities require additional effort for target development to make them withstand the increased energy deposit [119].

There is a variety of such installations available at accelerator facilities worldwide. Some of the research teams focus on the quest for the discovery of new elements following traditional pathways, e.g., at the gas-filled separators DGFRS [120] of FLNR/JINR in Dubna, Russia, or GARIS at RIKEN in Wako, Japan [121]. Other facilities have changed their focus to novel techniques like ion traps for high-precision mass measurements and laser spectroscopy like the velocity filter SHIP of GSI/FAIR, Darmstadt, Germany. Nuclear spectroscopy, in-beam and, in particular, decay spectroscopy after separation (DSAS), needed for the investigation of meta-stable nuclear states in SHN is presently being performed at installations like the mass spectrometer FMA [122] and the gas-filled separator AGFA [123] at ANL in Lemont, IL, U.S.A., RITU [124] at the cyclotron laboratory of the University of Jyväskylä in Finland, the gas-filled separator BGS equipped with the FIONA mass separator at LBNL, Berkeley, CA, U.S.A. [125], the gas-filled separator TASCA at GSI/FAIR [126] and the velocity filter SHELS at FLNR/JINR, Dubna, Russia [127].

The major aim of future facilities aiming at SHN research is dictated by the ever lower cross sections for the investigation of ever heavier systems both, in terms of the synthesis of new heavy elements as well as for extending nuclear and atomic structure studies (in-beam and DSAS). The detailed knowledge of atomic and nuclear properties like binding energies, ionization potentials and atomic excitation levels, as well as the single-particle and collective nuclear excitations, are essential for a successful progress toward the eventual localization of the next proton and neutron shell closures. But the foremost important aim is the understanding of the strong interaction, promising a detailed insight into fundamental physics. As the first of the next-generation high-intensity stable beam facilities the SHE-factory of FLNR/JINR with the new gas-filled separator DGFRS2-2 [128] has started operation recently, while there are two other installations aiming at similar performance. While the HELIAC project of GSI/FAIR is still in an early stage with the first components being tested, the SPIRAL2 LINAC at GANIL has started operation of its first phase being limited for the highest intensities to projectile masses $A \lessapprox 40$. The second phase with the new injector NEWGAIN [129] will then provide the highest intensities for all ions and together with the separator-spectrometer set-up S^3 [130] will be one of the worldwide most competitive facilities for the investigation of SHN. S^3 will be equipped with the detection array for Spectroscopy and Identification of Rare Isotopes Using S^3 (SIRIUS) as well as the S^3 Low Energy Branch (S^3 LEB) [131] offering tools for laser spectroscopy, mass measurement and the set-up for laser/trap-assisted DSAS SEASON.

The results for the heaviest nuclei discussed in this review indicate the possible benefit of accessing extremely short lifetimes and the finest energy differences. These new experimental setups with their improved performance are, therefore, expected to have the potential to reach quantum features at the extremes of spin, lifetime and excitation energy.

Acknowledgements SA acknowledges the support from the Scientific Grant Agency VEGA (Contract No. 1/0651/21), and the Slovak Research and Development Agency (Contract No. APVV-22-0282).

Funding Open Access funding enabled and organized by Projekt DEAL.

Data availability No data are associated in the manuscript.

References

1. H. Meldner, Ark. Fys. **36**, 593 (1967)
2. A. Sobiczewski, F.A. Gareev, B.N. Kalinkin, Phys. Lett. **22**, 500 (1966), https://www.sciencedirect.com/science/article/abs/pii/0031916366912431

3. C.E. Düllmann, R.-D. Herzberg, W. Nazarewicz, Y. Oganessian, eds., Special Issue on Superheavy Elements, vol. 944 (Elsevier, B.V., 2015), https://www.sciencedirect.com/journal/nuclear-physics-a/vol/944/suppl/C
4. Y.T. Oganessian, A. Sobiczewski, G.M. Ter-Akopian, Phys. Scr. **92**, 023003 (2017). https://doi.org/10.1088/1402-4896/aa53c1
5. M. Leino, F. Heßberger, Annu. Rev. Nucl. Part. Sci. **54**, 175 (2004). https://doi.org/10.1146/annurev.nucl.53.041002.110332
6. R.-D. Herzberg, P. Greenlees, Progress in Particle and Nuclear Physics **61**, 674 (2008), ISSN 0146-6410, https://www.sciencedirect.com/science/article/pii/S0146641008000409
7. D. Ackermann, C. Theisen, Phys. Scr. **92**, 083002 (2017). https://doi.org/10.1088/1402-4896/aa7921
8. F.P. Heßberger, The European Physical Journal A **53**, 75 (2017). https://doi.org/10.1140/epja/i2017-12260-3
9. P.T. Greenlees, R.-D. Herzberg, S. Ketelhut, P.A. Butler, P. Chowdhury, T. Grahn, C. Gray-Jones, G.D. Jones, P. Jones, R. Julin et al., Phys. Rev. C **78**, 021303 (2008). https://doi.org/10.1103/PhysRevC.78.021303
10. C.F. Weizsäcker, Naturwissenschaften **24**, 813 (1936). https://doi.org/10.1007/BF01497732
11. O. Hahn, Naturwissenschaften **9**, 84 (1921), ISSN 1432-1904, https://doi.org/10.1007/BF01491321
12. P. Walker, Z. Podolyák, Phys. Scr. **95**, 044004 (2020). https://doi.org/10.1088/1402-4896/ab635d
13. K. Fajans, O. Göhring, PhysikalischeZeitschrift **14**, 877 (1913)
14. G.D. Dracoulis, P.M. Walker, F.G. Kondev, Reports on Progress in Physics **79**, 076301 (2016). http://stacks.iop.org/0034-4885/79/i=7/a=076301
15. R.R. Chasman, I. Ahmad, A.M. Friedman, J.R. Erskine, Rev. Mod. Phys. **49**, 833 (1977). https://doi.org/10.1103/RevModPhys.49.833
16. F. Kondev, G. Dracoulis, T. Kibédi, Atomic Data and Nuclear Data Tables **103–104**, 50 (2015), ISSN 0092-640X, http://www.sciencedirect.com/science/article/pii/S0092640X15000029
17. K. Löbner, Physics Letters B **26**, 369 (1968), ISSN 0370-2693, https://www.sciencedirect.com/science/article/pii/037026936890614X
18. P. Walker, G. Dracoulis, Nature **399**, 35 (1999). https://doi.org/10.1038/19911
19. P.F. Dittner, C.E. Bemis, D.C. Hensley, R.J. Silva, C.D. Goodman, Phys. Rev. Lett. **26**, 1037 (1971). https://doi.org/10.1103/PhysRevLett.26.1037
20. A. Ghiorso, K. Eskola, P. Eskola, M. Nurmia, Phys. Rev. C **7**, 2032 (1973). https://doi.org/10.1103/PhysRevC.7.2032
21. S. Hofmann, G. Münzenberg, Rev. Mod. Phys. **72**, 733 (2000). https://doi.org/10.1103/RevModPhys.72.733
22. S. Hofmann, F.P. Heßberger, D. Ackermann, S. Antalic, P. Cagarda, S. Ćwiok, B. Kindler, J. Kojouharova, B. Lommel, R. Mann et al., Eur. Phys. J. A **10**, 5 (2001). https://doi.org/10.1007/s100500170137
23. S. Antalic, F.P. Heßberger, S. Hofmann, D. Ackermann, S. Heinz, B. Kindler, I. Kojouharov, P. Kuusiniemi, M. Leino, B. Lommel, et al., Eur. Phys. J. A **43**, 35 (2010), ISSN 1434-601X. https://doi.org/10.1140/epja/i2009-10896-0
24. F.P. Heßberger, S. Antalic, F. Giacoppo, B. Andel, D. Ackermann, M. Block, S. Heinz, J. Khuyagbaatar, I. Kojouharov, M. Venhart, Eur. Phys. J. A **58**, 11 (2022). https://doi.org/10.1140/epja/s10050-022-00663-4
25. A. Chatillon, C. Theisen, P.T. Greenlees, G. Auger, J.E. Bastin, E. Bouchez, B. Bouriquet, J.M. Casandjian, R. Cee, E. Clément et al., The European Physical Journal A - Hadrons and Nuclei **30**, 397 (2006). https://doi.org/10.1140/epja/i2006-10134-5
26. S. Antalic, F.P. Heßberger, S. Hofmann, D. Ackermann, S. Heinz, B. Kindler, I. Kojouharov, P. Kuusiniemi, M. Leino, B. Lommel et al., The European Physical Journal A **38**, 219 (2008). https://doi.org/10.1140/epja/i2008-10665-7
27. F.P. Heßberger, S. Antalic, A.K. Mistry, D. Ackermann, B. Andel, M. Block, Z. Kalaninova, B. Kindler, I. Kojouharov, M. Laatiaoui et al., Eur. Phys. J. A **52**, 192 (2016). https://doi.org/10.1140/epja/i2016-16192-0
28. K. Hauschild, A. Lopez-Martens, R. Chakma, M.L. Chelnokov, V.I. Chepigin, A.V. Isaev, I.N. Izosimov, D.E. Katrasev, A.A. Kuznetsova, O.N. Malyshev et al., The European Physical Journal A **58**, 6 (2022). https://doi.org/10.1140/epja/s10050-021-00657-8
29. B. Streicher, F.P. Heßberger, S. Antalic, S. Hofmann, D. Ackermann, S. Heinz, B. Kindler, J. Khuyagbaatar, I. Kojouharov, P. Kuusiniemi et al., The European Physical Journal A **45**, 275 (2010). https://doi.org/10.1140/epja/i2010-11005-2
30. C. Bemis, R. Silva, D. Hensley, O.K. Jr., J. Tarrant, L. Hunt, P. Dittner, R. Hahn, C. Goodman, Tech. Rep.ORNL-4976 1973 page 37, 3ORNL (1974)
31. B. Štreicher, Ph.D. thesis, Comenius University Bratislava (2006). http://sok11249.dnp.fmph.uniba.sk/sok11249/?cont=prace&id=44
32. B. Štreicher, S. Antalic, v. Šaro, F. Heßberger, S. Hofmann, D. Ackermann, B. Kindler, I. Kojouharov, B. Lommel, R. Mann, et al., Acta Phys. Pol. B **38**, Ackermann, B. Kindler I. Kojouharov, B. Lommel, R. Mann, B. Sulignano (2007). https://www.actaphys.uj.edu.pl/fulltext?series=Reg &vol=38 &page=1561
33. A. Lopez-Martens, K. Hauschild, A.V. Yeremin, O. Dorvaux, A.V. Belozerov, C. Briançon, M.L. Chelnokov, V.I. Chepigin, D. Curien, P. Désesquelles et al., The European Physical Journal A **32**, 245 (2007). https://doi.org/10.1140/epja/i2007-10391-8
34. F.P. Heßberger, S. Antalic, D. Ackermann, B. Andel, M. Block, Z. Kalaninova, B. Kindler, I. Kojouharov, M. Laatiaoui, B. Lommel et al., Eur. Phys. J. A **52**, 328 (2016). https://doi.org/10.1140/epja/i2016-16328-2
35. S. Hofmann, G. Münzenberg, W. Faust, T. Kitahara, W. Reisdorf, P. Armbruster, K. Güttner, B. Thuma, GSI Scientific Report **1978**, 65 (1979)

36. G. Jones, Nuclear Instruments and Methods in Physics Research Section A: Accelerators, Spectrometers, Detectors and Associated Equipment **488**, 471 (2002), ISSN 0168-9002, https://www.sciencedirect.com/science/article/pii/S0168900202004692
37. S. Antalic, F.P. Heßberger, D. Ackermann, S. Heinz, S. Hofmann, Z. Kalaninová, B. Kindler, J. Khuyagbaatar, I. Kojouharov, P. Kuusiniemi et al., The European Physical Journal A **47**, 62 (2011). https://doi.org/10.1140/epja/i2011-11062-y
38. V.T. Jordanov, G.F. Knoll, Nucl. Instr. and Meth. A **345**, 337 (1994), https://www.sciencedirect.com/science/article/pii/0168900294910111
39. H.M. David, J. Chen, D. Seweryniak, F.G. Kondev, J.M. Gates, K.E. Gregorich, I. Ahmad, M. Albers, M. Alcorta, B.B. Back et al., Phys. Rev. Lett. **115**, 132502 (2015). https://doi.org/10.1103/PhysRevLett.115.132502
40. J. Kallunkathariyil, B. Sulignano, P.T. Greenlees, J. Khuyagbaatar, C. Theisen, K. Auranen, H. Badran, F. Bisso, P. Brionnet, R. Briselet et al., Phys. Rev. C **101**, 011301 (2020). https://doi.org/10.1103/PhysRevC.101.011301
41. J. Khuyagbaatar, H. Brand, C.E. Düllmann, F.P. Heßberger, E. Jäger, B. Kindler, J. Krier, N. Kurz, B. Lommel, Y. Nechiporenko et al., Phys. Rev. C **106**, 024309 (2022). https://doi.org/10.1103/PhysRevC.106.024309
42. A.V. Belozerov, M.L. Chelnokov, V.I. Chepigin, T.P. Drobina, V.A. Gorshkov, A.P. Kabachenko, O.N. Malyshev, I.M. Merkin, Y.T. Oganessian, A.G. Popeko et al., The European Physical Journal A - Hadrons and Nuclei **16**, 447 (2003). https://doi.org/10.1140/epja/i2002-10109-6
43. A. Robinson, T. Khoo, I. Ahmad, S. Tandel, F. Kondev, T. Nakasukasa, D. Seweryniak, M. Asai, B. Back, M. Carpenter et al., Phys. Rev. C **78**, 034308 (2008)
44. M. Block, F. Giacoppo, F.-P. Heßberger, S. Raeder, La Rivista del Nuovo Cimento **45**, 279 (2022). https://doi.org/10.1007/s40766-022-00030-5
45. A. Parkhomenko, A. Sobiczewski, Acta Phys. Pol. B **35**, 2447 (2004), https://www.actaphys.uj.edu.pl/fulltext?series=Reg&vol=35&page=2447
46. V. Ninov, F.P. Heßberger, S. Hofmann, H. Folger, G. Münzenberg, P. Armbruster, A.V. Yeremin, A.G. Popeko, M. Leino, S. Saro, Zeitschrift für Physik A Hadrons and Nuclei **356**, 11 (1996). https://doi.org/10.1007/s002180050141
47. G. Münzenberg, S. Hofmann, W. Faust, F.P. Heßberger, W. Reisdorf, K.H. Schmidt, T. Kitahara, P. Armbruster, K. Güttner, B. Thuma et al., Zeitschrift für Physik A Atoms and Nuclei **302**, 7 (1981). https://doi.org/10.1007/BF01425097
48. S. Hofmann, V. Ninov, F. Heßberger, H. Folger, G. Münzenberg, H. Schött, P. Armbruster, A. Andreyev, A. Popeko, A. Yeremin et al., GSI Ann. Rep. **1993**, 64 (1994)
49. F.P. Heßberger, S. Antalic, B. Streicher, S. Hofmann, D. Ackermann, B. Kindler, I. Kojouharov, P. Kuusiniemi, M. Leino, B. Lommel et al., The European Physical Journal A - Hadrons and Nuclei **26**, 233 (2005). https://doi.org/10.1140/epja/i2005-10171-6
50. S. Ćwiok, S. Hofmann, and W. Nazarewicz, Nucl. Phys. A **573**, 356 (1994), ISSN 0375-9474. http://www.sciencedirect.com/science/article/pii/0375947494903492
51. F.P. Heßberger, S. Hofmann, D. Ackermann, V. Ninov, M. Leino, G. Münzenberg, S. Saro, A. Lavrentev, A.G. Popeko, A.V. Yeremin et al., Eur. Phys. J. A **12**, 57 (2001). https://doi.org/10.1007/s100500170039
52. E. Browne, J. Tuli, Nuclear Data Sheets **114**, 1041 (2013), ISSN 0090-3752, https://www.sciencedirect.com/science/article/pii/S0090375213000549
53. B. Buck, A.C. Merchant, S.M. Perez, J. Phys. G: Nucl. Part. Phys. **18**, 143 (1992). https://doi.org/10.1088/0954-3899/18/1/012
54. T. Huang, D. Seweryniak, B.B. Back, P.C. Bender, M.P. Carpenter, P. Chowdhury, R.M. Clark, P.A. Copp, X.-T. He, R.D. Herzberg et al., Phys. Rev. C **106**, L061301 (2022). https://doi.org/10.1103/PhysRevC.106.L061301
55. F.P. Heßberger, EPJ Web Conf. **131**, 02005 (2016). https://doi.org/10.1051/epjconf/201613102005
56. U. Forsberg, D. Rudolph, L.-L. Andersson, A. Di Nitto, C. Düllmann, C. Fahlander, J. Gates, P. Golubev, K. Gregorich, C. Gross, et al., Nuclear Physics A **953**, 117 (2016), ISSN 0375-9474, https://www.sciencedirect.com/science/article/pii/S0375947416300768
57. P.M. Walker, F.G. Kondev, The European Physical Journal Special Topics (2024). https://doi.org/10.1140/epjs/s11734-024-01096-4
58. L.P. Somerville, M.J. Nurmia, J.M. Nitschke, A. Ghiorso, E.K. Hulet, R.W. Lougheed, Phys. Rev. C **31**, 1801 (1985). https://doi.org/10.1103/PhysRevC.31.1801
59. M.R. Lane, K.E. Gregorich, D.M. Lee, M.F. Mohar, M. Hsu, C.D. Kacher, B. Kadkhodayan, M.P. Neu, N.J. Stoyer, E.R. Sylwester et al., Phys. Rev. C **53**, 2893 (1996). https://doi.org/10.1103/PhysRevC.53.2893
60. D. Ackermann, Nucl. Phys. A **944**, 376 (2015). ISSN 0375-9474, http://www.sciencedirect.com/science/article/pii/S0375947415002018
61. R.W. Hoff, T. von Egidy, R.W. Lougheed, D.H. White, H.G. Börner, K. Schreckenbach, G. Barreau, D.D. Warner, Phys. Rev. C **29**, 618 (1984). https://doi.org/10.1103/PhysRevC.29.618
62. P.G. Hansen, K. Wilsky, C.V.K. Baba, S.E. Vandenbosch, Nuclear Physics **45**, 410 (1963), ISSN 0029-5582, https://orbit.dtu.dk/en/publications/decay-of-an-isomeric-state-in-cm244
63. L.G. Multhauf, K.G. Tirsell, R.A. Meyer, Phys. Rev. C **13**, 771 (1976). https://doi.org/10.1103/PhysRevC.13.771
64. R. Orlandi, H. Makii, K. Nishio, K. Hirose, M. Asai, K. Tsukada, T.K. Sato, Y. Ito, F. Suzaki, Y. Nagame et al., Phys. Rev. C **106**, 064301 (2022). https://doi.org/10.1103/PhysRevC.106.064301
65. S. Ketelhut, Ph.D. thesis, University of Jyväskylä (2010)

66. R.-D. Herzberg, D.M. Cox, Radiochim. Acta **99**, 441 (2011). https://doi.org/10.1524/ract.2011.1858
67. H.L. Liu, P.M. Walker, F.R. Xu, Phys. Rev. C **89**, 044304 (2014). https://doi.org/10.1103/PhysRevC.89.044304
68. H.L. Hall, K.E. Gregorich, R.A. Henderson, D.M. Lee, D.C. Hoffman, M.E. Bunker, M.M. Fowler, P. Lysaght, J.W. Starner, J.B. Wilhelmy, Phys. Rev. C **39**, 1866 (1989). https://doi.org/10.1103/PhysRevC.39.1866
69. T. Goigoux, C. Theisen, B. Sulignano, M. Airiau, K. Auranen, H. Badran, R. Briselet, T. Calverley, D. Cox, F. Déchery et al., Eur. Phys. J. A **57**, 321 (2021). https://doi.org/10.1140/epja/s10050-021-00631-4
70. D. Peterson, B.B. Back, R.V.F. Janssens, T.L. Khoo, C.J. Lister, D. Seweryniak, I. Ahmad, M.P. Carpenter, C.N. Davids, A.A. Hecht et al., Phys. Rev. C **74**, 014316 (2006). https://doi.org/10.1103/PhysRevC.74.014316
71. F.P. Heßberger, S. Hofmann, D. Ackermann, S. Antalic, B. Kindler, I. Kojouharov, P. Kuusiniemi, M. Leino, B. Lommel, R. Mann et al., The European Physical Journal A - Hadrons and Nuclei **30**, 561 (2006). https://doi.org/10.1140/epja/i2006-10137-2
72. A. Lopez-Martens, K. Hauschild, A.I. Svirikhin, Z. Asfari, M.L. Chelnokov, V.I. Chepigin, O. Dorvaux, M. Forge, B. Gall, A.V. Isaev et al., Phys. Rev. C **105**, L021306 (2022). https://doi.org/10.1103/PhysRevC.105.L021306
73. B. Sulignano, S. Heinz, F.P. Heßberger, S. Hofmann, D. Ackermann, S. Antalic, B. Kindler, I. Kojouharov, P. Kuusiniemi, B. Lommel et al., The European Physical Journal A **33**, 327 (2007). https://doi.org/10.1140/epja/i2007-10469-3
74. B. Sulignano, C. Theisen, J.-P. Delaroche, M. Girod, J. Ljungvall, D. Ackermann, S. Antalic, O. Dorvaux, A. Drouart, B. Gall et al., Phys. Rev. C **86**, 044318 (2012). https://doi.org/10.1103/PhysRevC.86.044318
75. R.D. Herzberg, P.T. Greenlees, P.A. Butler, G.D. Jones, M. Venhart, I.G. Darby, S. Eeckhaudt, K. Eskola, T. Grahn, C. Gray-Jones et al., Nature **442**, 896 (2006). https://doi.org/10.1038/nature05069
76. S.K. Tandel, T.L. Khoo, D. Seweryniak, G. Mukherjee, I. Ahmad, B. Back, R. Blinstrup, M. Carpenter, J. Chapman, P. Chowdhury et al., Phys. Rev. Lett. **97**, 082502 (2006). https://doi.org/10.1103/PhysRevLett.97.082502
77. R. Clark, K. Gregorich, J. Berryman, M. Ali, J. Allmond, C. Beausang, M. Cromaz, M. Deleplanque, I. Dragojević, J. Dvorak, et al., Physics Letters B **690**, 19 (2010). ISSN 0370-2693, https://www.sciencedirect.com/science/article/pii/S0370269310005757
78. F.P. Heßberger, S. Antalic, B. Sulignano, D. Ackermann, S. Heinz, S. Hofmann, B. Kindler, J. Khuyagbaatar, I. Kojouharov, P. Kuusiniemi et al., The European Physical Journal A **43**, 55 (2010). https://doi.org/10.1140/epja/i2009-10899-9
79. A. Bronis, F.P. Heßberger, S. Antalic, B. Andel, D. Ackermann, S. Heinz, S. Hofmann, J. Khuyagbaatar, B. Kindler, I. Kojouharov et al., Phys. Rev. C **106**, 014602 (2022). https://doi.org/10.1103/PhysRevC.106.014602
80. K. Kessaci, Ph.D. thesis, l'Université de Strasbourg (2022). https://www.theses.fr/s269617
81. K. Kessaci, B.J.P. Gall, O. Dorvaux, A. Lopez-Martens, R. Chakma, K. Hauschild, M.L. Chelnokov, V.I. Chepigin, M. Forge, A.V. Isaev et al., Phys. Rev. C **104**, 044609 (2021). https://doi.org/10.1103/PhysRevC.104.044609
82. H.B. Jeppesen, R.M. Clark, K.E. Gregorich, A.V. Afanasjev, M.N. Ali, J.M. Allmond, C.W. Beausang, M. Cromaz, M.A. Deleplanque, I. Dragojević et al., Phys. Rev. C **80**, 034324 (2009). https://doi.org/10.1103/PhysRevC.80.034324
83. K. Hauschild, A. Lopez-Martens, A.V. Yeremin, O. Dorvaux, S. Antalic, A.V. Belozerov, C. Briançon, M.L. Chelnokov, V.I. Chepigin, D. Curien et al., Phys. Rev. C **78**, 021302 (2008). https://doi.org/10.1103/PhysRevC.78.021302
84. J. Khuyagbaatar, H. Brand, R.A. Cantemir, C.E. Düllmann, F.P. Heßberger, E. Jäger, B. Kindler, J. Krier, N. Kurz, B. Lommel et al., Phys. Rev. C **104**, L031303 (2021). https://doi.org/10.1103/PhysRevC.104.L031303
85. P. Mosat, S. Antalic, F.P. Heßberger, D. Ackermann, B. Andel, M.S. Block, Z. Kalaninova, B. Kindler, M. Laatiaoui, B. Lommel, et al., Acta Phys. Pol. B **51**, 849 (2020). https://www.actaphys.uj.edu.pl/R/51/3/849
86. R. Chakma, A. Lopez-Martens, K. Hauschild, A.V. Yeremin, O.N. Malyshev, A.G. Popeko, Y.A. Popov, A.I. Svirikhin, V.I. Chepigin, E.A. Sokol et al., Phys. Rev. C **107**, 014326 (2023). https://doi.org/10.1103/PhysRevC.107.014326
87. H.B. Jeppesen, I. Dragojević, R.M. Clark, K.E. Gregorich, M.N. Ali, J.M. Allmond, C.W. Beausang, D.L. Bleuel, M. Cromaz, M.A. Deleplanque et al., Phys. Rev. C **79**, 031303 (2009). https://doi.org/10.1103/PhysRevC.79.031303
88. J.S. Berryman, R.M. Clark, K.E. Gregorich, J.M. Allmond, D.L. Bleuel, M. Cromaz, I. Dragojević, J. Dvorak, P.A. Ellison, P. Fallon et al., Phys. Rev. C **81**, 064325 (2010). https://doi.org/10.1103/PhysRevC.81.064325
89. J. Qian, A. Heinz, T.L. Khoo, R.V.F. Janssens, D. Peterson, D. Seweryniak, I. Ahmad, M. Asai, B.B. Back, M.P. Carpenter et al., Phys. Rev. C **79**, 064319 (2009). https://doi.org/10.1103/PhysRevC.79.064319
90. J. Rissanen, R.M. Clark, K.E. Gregorich, J.M. Gates, C.M. Campbell, H.L. Crawford, M. Cromaz, N.E. Esker, P. Fallon, U. Forsberg et al., Phys. Rev. C **88**, 044313 (2013). https://doi.org/10.1103/PhysRevC.88.044313
91. D. Ackermann, F.P. Heßberger, S. Antalic, M. Block, H.-G. Burkhard, V.F. Comas, P.T. Greenlees, S. Heinz, S. Hofmann, S. Ketelhut et al., GSI Sci. Rep. **2011**, 208 (2012)
92. A. Parkhomenko and A. Sobiczewski, Acta Phys. Pol. B **36**, 3095 (2005). https://www.actaphys.uj.edu.pl/fulltext?series=Reg&vol=36&page=3115
93. T. Ishii, H. Makii, M. Asai, K. Tsukada, A. Toyoshima, M. Matsuda, A. Makishima, S. Shigematsu, J. Kaneko, T. Shizuma et al., Phys. Rev. C **78**, 054309 (2008). https://doi.org/10.1103/PhysRevC.78.054309
94. S. Antalic, F.P. Heßberger, D. Ackermann, S. Heinz, S. Hofmann, B. Kindler, J. Khuyagbaatar, B. Lommel, R. Mann, Eur. Phys. J. A **51**, 41 (2015). https://doi.org/10.1140/epja/i2015-15041-0
95. J.-P. Delaroche, M. Girod, H. Goutte, J. Libert, Nuclear Physics A **771**, 103 (2006), ISSN 0375-9474, https://www.sciencedirect.com/science/article/pii/S0375947406001291
96. G. Adamian, N. Antonenko, W. Scheid, Phys. Rev. C **81**, 024320 (2010). https://doi.org/10.1103/PhysRevC.81.024320

97. N. Minkov, L. Bonneau, P. Quentin, J. Bartel, H. Molique, D. Ivanova, Phys. Rev. C **105**, 044329 (2022). https://doi.org/10.1103/PhysRevC.105.044329
98. F.R. Xu, E.G. Zhao, R. Wyss, P.M. Walker, Phys. Rev. Lett. **92**, 252501 (2004). https://doi.org/10.1103/PhysRevLett.92.252501
99. V.I. Zagrebaev, W. Greiner, Phys. Rev. C **83**, 044618 (2011). https://doi.org/10.1103/PhysRevC.83.044618
100. V.I. Zagrebaev, W. Greiner, Phys. Rev. C **87**, 034608 (2013). https://doi.org/10.1103/PhysRevC.87.034608
101. V. Saiko, A. Karpov, European Physical Journal A – Hadrons & Nuclei **58**, 1 (2022), https://search.ebscohost.com/login.aspx?direct=true&db=a9h&AN=156317391&lang=fr&site=ehost-live
102. M. Asai, K. Tsukada, Y. Kasamatsu, T. Sato, A. Toyoshima, Y. Ishii, R. Takahashi, Y. Nagame, T. Ishii, I. Nishinaka, et al., JAEA-Review 2009-036 page 37,JAEA-Tokai Tandem Annual Report (2009). https://jopss.jaea.go.jp/pdfdata/JAEA-Review-2009-036.pdf
103. P. Möller, A. Sierk, T. Ichikawa, H. Sagawa, At. Data and Nucl. Data Tables **109-110**, 1 (2016), ISSN 0092-640X, https://www.sciencedirect.com/science/article/pii/S0092640X1600005X
104. M. Asai, K. Tsukada, H. Haba, Y. Ishii, T. Ichikawa, A. Toyoshima, T. Ishii, Y. Nagame, I. Nishinaka, Y. Kojima et al., Phys. Rev. C **83**, 014315 (2011). https://doi.org/10.1103/PhysRevC.83.014315
105. R. Briselet, C. Theisen, M. Vandebrouck, A. Marchix, M. Airiau, K. Auranen, H. Badran, D. Boilley, T. Calverley, D. Cox et al., Phys. Rev. C **99**, 024614 (2019). https://doi.org/10.1103/PhysRevC.99.024614
106. R. Briselet, C. Theisen, B. Sulignano, M. Airiau, K. Auranen, D.M. Cox, F. Déchery, A. Drouart, Z. Favier, B. Gall et al., Phys. Rev. C **102**, 014307 (2020). https://doi.org/10.1103/PhysRevC.102.014307
107. I. Muntian, Z. Patyk, A. Sobiczewski, Physics Letters B **500**, 241 (2001). ISSN 0370-2693, http://www.sciencedirect.com/science/article/pii/S0370269301000909
108. H.J. Krappe, J.R. Nix, A.J. Sierk, Phys. Rev. C **20**, 992 (1979). https://doi.org/10.1103/PhysRevC.20.992
109. S. Cwiok, J. Dudek, W. Nazarewicz, J. Skalski, T. Werner, Computer Physics Communications **46**, 379 (1987). ISSN 0010-4655, https://www.sciencedirect.com/science/article/pii/0010465587900932
110. M. Vostinar, F.P. Heßberger, D. Ackermann, B. Andel, S. Antalic, M. Block, C. Droese, J. Even, S. Heinz, Z. Kalaninova et al., Eur. Phys. J. A **55**, 17 (2019). https://doi.org/10.1140/epja/i2019-12701-y
111. S.A. Johansson, Nuclear Physics **12**, 449 (1959). ISSN 0029-5582, https://www.sciencedirect.com/science/article/pii/0029558259900203
112. J. Randrup, C. Tsang, P. Möller, S. Nilsson, S. Larsson, Nuclear Physics A **217**, 221 (1973). ISSN 0375-9474, https://www.sciencedirect.com/science/article/pii/0375947473901929
113. A. Lopez-Martens, K. Hauschild, A.I. Svirikhin, Z. Asfari, M.L. Chelnokov, V.I. Chepigin, O. Dorvaux, M. Forge, B. Gall, A.V. Isaev et al., EPJ Web of Conf. **290**, 02027 (2023). https://doi.org/10.1051/epjconf/202329002027
114. V. Viola, B. Wilkins, Nucl. Phys. **82**, 65 (1966)
115. J. Khuyagbaatar, The European Physical Journal A **58**, 243 (2022). https://doi.org/10.1140/epja/s10050-022-00896-3
116. F.P. Heßberger, K Isomers in Transuranium Nuclei (2023). https://arxiv.org/abs/2309.10468
117. F.P. Heßberger, S. Hofmann, V. Ninov, P. Armbruster, H. Folger, G. Münzenberg, H.J. Schött, A.G. Popeko, A.V. Yeremin, A.N. Andreyev et al., Zeitschrift für Physik A Hadrons and Nuclei **359**, 415 (1997). ISSN 1431-5831, https://doi.org/10.1007/s002180050422
118. D.S. Delion, R.J. Liotta, R. Wyss, Phys. Rev. C **76**, 044301 (2007). https://doi.org/10.1103/PhysRevC.76.044301
119. C. Stodel, J.F. Libin, C. Marry, F. Lutton, M.G. Saint-Laurent, B. Bastin, J. Piot, E. Clement, S. Le Moal, V. Morel et al., J. Radioanal. Nucl. Chem. **305**, 761 (2015). https://doi.org/10.1007/s10967-015-3936-5
120. Y.S. Tsyganov, J. Phys. G: Nucl. Part. Phys. **25**, 937 (1999). https://doi.org/10.1088/0954-3899/25/4/074
121. K. Morita, A. Yoshida, T. Inamura, M. Koizumi, T. Nomura, M. Fujioka, T. Shinozuka, H. Miyatake, K. Sueki, H. Kudo et al., Nuclear Instruments and Methods in Physics Research Section B: Beam Interactions with Materials and Atoms **70**, 220 (1992). ISSN 0168-583X, https://www.sciencedirect.com/science/article/pii/0168583X9295935K
122. C.N. Davids, J.D. Larson, Nuclear Instruments and Methods in Physics Research Section B: Beam Interactions with Materials and Atoms **40-41**, 1224 (1989). ISSN 0168-583X, https://www.sciencedirect.com/science/article/pii/0168583X89906241
123. D. Seweryniak, Nucl. Inst. Meth. B **317, Part B**, 274 (2013). ISSN 0168-583X, XVIth International Conference on ElectroMagnetic Isotope Separators and Techniques Related to their Applications, December 27, 2012 at Matsue, Japan, http://www.sciencedirect.com/science/article/pii/S0168583X13008215
124. M. Leino, J. Äystö, T. Enqvist, P. Heikkinen, A. Jokinen, M. Nurmia, A. Ostrowski, W. Trzaska, J. Uusitalo, K. Eskola et al., Nuclear Instruments and Methods in Physics Research Section B: Beam Interactions with Materials and Atoms **99**, 653 (1995). ISSN 0168-583X, application of Accelerators in Research and Industry '94, https://www.sciencedirect.com/science/article/pii/0168583X94005737
125. J.M. Gates, J. L. Pore, Eur. Phys. J. A **58**, 1 (2022). ISSN 14346001, https://search-ebscohost-com.in2p3.bib.cnrs.fr/login.aspx?direct=true&db=a9h&AN=160254331&lang=fr&site=ehost-live
126. A. Semchenkov, W. Brüchle, E. Jäger, E. Schimpf, M. Schädel, C.Mühle, F. Klos, A. TÃürler, A. Yakushev, A. Belov et al., Nucl. Instr. and Meth. B **266**, 4153 (2008)
127. A. Yeremin, O. Malyshev, A. Popeko, V. Chepigin, A. Svirikhin, A. Lopez-Martens, K. Hauschild, O. Dorvaux, B. Gall, J. Gehlot, EPJ Web of Conferences **86**, 00065 (2015). https://doi.org/10.1051/epjconf/20158600065

128. Y. Oganessian, V. Utyonkov, A. Popeko, D. Solovyev, F. Abdullin, S. Dmitriev, D. Ibadullayev, M. Itkis, N. Kovrizhnykh, D. Kuznetsov et al., Nuclear Instruments and Methods in Physics Research Section A: Accelerators, Spectrometers, Detectors and Associated Equipment **1033**, 166640 (2022), ISSN 0168-9002, https://www.sciencedirect.com/science/article/pii/S0168900222002078
129. D. Ackermann, B. Blank, L. Caceres, M. Caamaño, G. De France, B. Gall, S. Grévy, C. Grygiel, E. Lamour, X. Ledoux, et al., Technical Report, GANIL - document link: https://www.ganil-spiral2.eu/scientists/ganil-spiral-2-facilities/accelerators/newgain/ (2021). https://hal.archives-ouvertes.fr/hal-03280595
130. F. Déchery, A. Drouart, H. Savajols, J. Nolen, M. Authier, A.M. Amthor, D. Boutin, O. Delferriére, B. Gall, A. Hue et al., Eur. Phys. J. A **51**, 1 (2015), ISSN 1434-601X, https://doi.org/10.1140/epja/i2015-15066-3
131. A. Ajayakumar, J. Romans, M. Authier, Y. Balasmeh, A. Brizard, F. Boumard, L. Caceres, J.-F. Cam, A. Claessens, S. Damoy et al., Nuclear Instruments and Methods in Physics Research Section B: Beam Interactions with Materials and Atoms **539**, 102 (2023), ISSN 0168-583X, https://www.sciencedirect.com/science/article/pii/S0168583X23001003